

UC Davis

UC Davis Previously Published Works

Title

Genomic responses to parallel temperature gradients in the eelgrass *Zostera marina* in adjacent bays

Permalink

<https://escholarship.org/uc/item/4384d5q8>

Journal

Molecular Ecology, 32(11)

ISSN

0962-1083

Authors

Schiebelhut, Lauren M
Grosberg, Richard K
Stachowicz, John J
[et al.](#)

Publication Date

2023-06-01

DOI

10.1111/mec.16899

Copyright Information

This work is made available under the terms of a Creative Commons Attribution-NonCommercial-NoDerivatives License, available at <https://creativecommons.org/licenses/by-nc-nd/4.0/>

Peer reviewed

MOLECULAR ECOLOGY**Genomic responses to parallel temperature gradients in the eelgrass *Zostera marina* in adjacent bays**

Journal:	<i>Molecular Ecology</i>
Manuscript ID	MEC-22-1114.R1
Manuscript Type:	Original Article
Date Submitted by the Author:	n/a
Complete List of Authors:	Schiebelhut, Lauren; University of California Merced, Life and Environmental Sciences Grosberg, Richard ; University of California Davis Stachowicz, Jay; University of California Davis Bay, Rachael; UC Davis,
Keywords:	non-parallel evolution, population genomics, <i>Zostera marina</i> , Population Genetics - Empirical

1 **Genomic responses to parallel temperature gradients in the eelgrass *Zostera marina* in**
2 **adjacent bays**

3 Lauren M. Schiebelhut¹, Richard K. Grosberg², & John J. Stachowicz², Rachael A. Bay²

4 ¹Life and Environmental Sciences, University of California, Merced, California

5 ²Department of Evolution and Ecology, University of California, Davis, California

6

7 **Abstract**

8 The extent of parallel genomic responses to similar selective pressures depends on a complex
9 array of environmental, demographic, and evolutionary forces. Laboratory experiments with
10 replicated selective pressures yield mixed outcomes under controlled conditions and our
11 understanding of genomic parallelism in the wild is limited to a few well-established systems.
12 Here, we examine genomic signals of selection in the eelgrass *Zostera marina* across
13 temperature gradients in adjacent embayments. Although we find many genomic regions with
14 signals of selection within each bay. However, there is very little overlap in signals of selection
15 at the SNP level, despite most polymorphisms being shared across bays. We do find overlap at
16 the gene level, potentially suggesting multiple mutational pathways to the same phenotype.
17 Using polygenic models we find that some sets of candidate SNPs are able to predict
18 temperature across both bays, suggesting that small but parallel shifts in allele frequencies may
19 be missed by independent genome scans. Together, these results highlight the continuous
20 rather than binary nature of parallel evolution in polygenic traits and the complexity of
21 evolutionary predictability.

22 **Keywords:** non-parallel evolution, population genomics, *Zostera marina*

23 Introduction

24 The question of whether patterns of trait and underlying genomic and developmental variation
25 show parallel (or convergent) responses across similar selection gradients is fundamental to our
26 understanding of how evolution operates and whether evolutionary outcomes are predictable
27 (reviewed in Bolnick, Barrett, Oke, Rennison, & Stuart, 2018). All else being equal (and
28 notwithstanding the stochastic effects of genetic drift), independent populations experiencing
29 comparable selective regimes should exhibit parallel responses, at least at the trait level. The
30 degree to which such populations share similar genetic histories should also govern the extent
31 to which they exhibit parallel responses at the genomic level (Härer, Bolnick, & Rennison, 2021;
32 Rennison, Delmore, Samuk, Owens, & Miller, 2020). Thus, populations most likely to evolve
33 along parallel evolutionary pathways should have recently diverged, sharing a similar pool of
34 ancestral genetic variation, and independently facing comparable forces of selection
35 (Bohutínská et al., 2021; Conte, Arnegard, Peichel, & Schluter, 2012).

36 The extent of parallelism in populations experiencing nominally comparable selective
37 regimes may also depend on the level of organization under consideration, from the traits
38 themselves, to underlying variation at the level of nucleotides, genes, and developmental
39 pathways (Bolnick et al., 2018; Conte et al., 2012; Stuart, 2019). For example, many selectively
40 important traits are highly polygenic, reducing the likelihood of parallelism at the
41 genetic/genomic level, with different genetic combinations producing functionally equivalent
42 phenotypes (Arendt & Reznick, 2008). In addition, there are often multiple phenotypic
43 solutions, some based on historical contingency, to the same selective challenges, with
44 different combinations of traits leading to a suite of phenotypes with similar performance

45 (Bolnick et al., 2018). Finally, non-parallel mutations in particular genes, or mutations within the
46 same class of genes (but not the same genes), may produce parallel phenotypic or functional
47 effects (e.g., Cassin-Sackett, Callicrate, & Fleischer, 2019; Rosenblum, Römpler, Schöneberg, &
48 Hoekstra, 2010).

49 In principle, the strongest tests for parallel evolution would use highly replicated
50 populations with known evolutionary histories inhabiting comparable selective regimes in
51 which patterns can be assayed at both the trait and genomic levels. For these reasons, the
52 majority of studies exploring parallelism of both genomes and traits have involved long-term
53 laboratory studies of microbes, often initiated from a single clone, and allowed to evolve over
54 thousands of generations under varying selective regimes (reviewed in Blount, Lenski, & Losos,
55 2018; also see Pickersgill (2018) for analysis of crop plants). Consistent with predictions, parallel
56 outcomes are most likely in recently established populations experiencing equivalent selective
57 regimes (e.g., Blount et al., 2018). Nevertheless, responses are often strikingly inconsistent
58 among replicate lines, even those initiated from the same founder and subjected to presumably
59 identical selective regimes (Tenailon et al., 2012). This suggests that stochastic processes such
60 as genetic drift, and the often complex relationships among genotypes, phenotypes and fitness
61 may also be shaping evolutionary responses at the genomic and trait levels (Conte et al., 2012).

62 Far less is known about evolutionary patterns in natural populations of multicellular
63 organisms (Blount et al., 2018; Bolnick et al., 2018). The majority of the data that we do have
64 from a few well-characterized model systems suggests that parallelism is equally inconsistent in
65 these systems (Stuart et al., 2017). However, recent advances in the accessibility of genomic
66 tools make it possible to simultaneously assess population structure and evolutionary history

67 while identifying specific mutations associated with parallel selection pressures. This allows for
68 studies of parallel evolution in “replicate” populations with unknown/uncertain evolutionary
69 histories and longer generation times and thereby extends these experimental studies to
70 natural populations of more complex non-model organisms. Several recent studies comparing
71 natural populations identified substantial degrees of parallelism both in terms of traits and
72 underlying genetic patterns (e.g., Bohutínská et al., 2021; Roda et al., 2013; Stuart et al., 2017);
73 however, as with several laboratory studies on microbes, in many wild populations multiple
74 factors, including genetic drift (Szendro, Franke, de Visser, & Krug, 2013), environmental
75 heterogeneity (Magalhaes et al., 2021; Stuart et al., 2017), and different histories of fluctuating
76 selection (Liu, Ferchaud, Grønkjaer, Nygaard, & Hansen, 2018) often contribute to varying
77 degrees of decoupling of parallelism between genes and traits (e.g., Rivas et al., 2018).

78 As the most widely distributed marine angiosperm in the northern hemisphere, the
79 seagrass *Zostera marina* occurs from the Arctic to the subtropics and in the Pacific, Atlantic and
80 the Mediterranean. The broad distribution of *Z. marina* encompasses a wide range of
81 environmental conditions (with respect to light, salinity, and temperature) that vary both
82 seasonally and geographically. *Z. marina* undergoes both vegetative and sexual reproduction,
83 with varying proportions across sites (Reusch et al., 1999; Olsen et al., 2004). In most
84 populations, individual shoots (ramets) derived from a sexually produced individual are
85 intermingled to form the seagrass meadow (see map in Kollars et al. 2022), with only a few
86 extreme exceptions (Yu et al. 2022). Clonal genotypes, even those collected from the same bed,
87 differ in fitness-related traits, including shoot production, biomass, photosynthesis, and
88 nutrient uptake (Abbott, DuBois, Grosberg, Williams, & Stachowicz, 2018; Hughes, Stachowicz,

89 & Williams, 2009; Reynolds, DuBois, Abbott, Williams, & Stachowicz, 2016; Salo, Reusch, &
90 Boström, 2015). However, the expression of these traits also depends on environmental
91 context, leading to differential fitness of genotypes at particular sites or seasons (DuBois,
92 Abbott, Williams, & Stachowicz, 2019; DuBois, Williams, & Stachowicz, 2021). This standing
93 genetic variation provides the foundation for local adaptation and reciprocal transplants have
94 demonstrated home-site advantage even at spatial scales on the order of a few km (DuBois,
95 Pollard, Kauffman, Williams, & Stachowicz, 2022; Hämmerli & Reusch, 2002). Moreover,
96 population structure in *Z. marina* tends to be high with significant divergence at all spatial
97 scales, including across tidal heights (Campanella, Bologna, Smith, Rosenzweig, & Smalley,
98 2010; DuBois et al., 2022; Kamel, Hughes, Grosberg, & Stachowicz, 2012; J. H. Kim et al., 2017),
99 so limited gene flow, even at the scale of meters, may facilitate local adaptation.

100 In this paper we simultaneously characterize patterns of genomic and functional
101 variation in multiple populations of *Z. marina*, across adjacent bays with overlapping thermal
102 gradients. We focus on populations of *Z. marina* inhabiting multiple locations along
103 temperature gradients in the adjacent Tomales Bay and Bodega Harbor in north-central
104 California, USA. These two bays are just 10 kilometers apart, making it likely that populations
105 within each bay arose from the same ancestral population. This, along with the overlapping
106 selective gradient (i.e., temperature) represents a set of conditions under which parallel
107 responses might be most likely. Previous work has demonstrated strong genetic structure in
108 this region, as well as local adaptation to temperature; reciprocal transplants in Tomales Bay
109 show home-site advantage and plants from cooler sites have decreased growth under
110 experimental warming (DuBois et al., 2022). Because of this strong population structure and

111 because warm sites in each embayment are farthest from the open sea and thus the most
112 distant from one another of all our sites, we can interpret parallel shifts in allele frequencies as
113 signatures of selection, relative to random processes such as genetic drift. We build on this
114 trait-based evidence of local adaptation to investigate the genomic basis of adaptation and the
115 potential for parallel evolution, focusing on three questions. We first ask whether genotype-
116 temperature associations exist across each temperature gradient independently and whether
117 there are parallel changes in allele frequencies across tidal heights. We then determine
118 whether parallelism at the genomic level exists across the two gradients, assessing overlap at
119 three levels of organization: the mutation, the gene, and the functional pathway. Finally, to
120 assess the predictability of detected genotype-temperature relationships, we test whether
121 genetic variation across many SNPs can be used to predict thermal environment from individual
122 genotypes, both within and between bays.

123

124 **Methods**

125

126 ***Sampling, DNA extraction, and sequencing***

127 For population genomic analyses, we collected 2-3 shoots attached by a rhizome from fifteen
128 putative genets (separated by approximately 5-10 m) at 14 sites across Tomales Bay and
129 Bodega Harbor in California (Table 1) from a height below 0.0 mean lower low water (MLLW)
130 (i.e., not sampling the uppermost or lowermost vertical distribution of *Z. marina*). At our study
131 sites (and throughout much of the Pacific Ocean) genets cover a relatively small area such that
132 ramets sampled 1 - 2m apart rarely include the same multi-locus genotype (Kamel et al. 2012;

133 Reynolds et al. 2017; Duffy et al. 2022; Kollars et al. 2022). For two of the sites sampled in
134 Bodega Harbor (Mason's Marina and Westside Park) we also collected a deeper set of
135 specimens (at least -0.6m below MLLW) to test for genetic differences between shallower
136 versus deeper plants. We transported plants back to the University of California, Davis in a
137 cooler with ice packs, and stored them for no more than one day in a recirculating seawater
138 table before dissecting out the tissue from within the leaf sheath of all shoots within a genet
139 and then flash-froze them in liquid nitrogen and stored at -80°C. Using the inner leaf sheath
140 tissue allowed us to minimize the amount of non-eelgrass DNA by selecting tissue that was free
141 of epibionts and had lower chloroplast concentrations.

142 We extracted DNA from up to 200 mg of frozen tissue by grinding with a plastic pestle
143 and liquid nitrogen in a 1.5 ml tube until powdered and then by using a modified CTAB
144 chloroform extraction (Doyle & Doyle, 1987). Briefly, tissue was resuspended in 800 ul CTAB
145 (0.1 M Tris-HCl [pH 8.0], 0.02 M EDTA [pH 8.0], 3% CTAB, 1.4 M NaCl, 0.2% β -mercaptoethanol),
146 after the first chloroform-isoamyl alcohol step, the upper aqueous phase was transferred to a
147 new tube and treated with 2 μ l of RNase A at 37°C for one hour, followed by an additional
148 chloroform-isoamyl alcohol step before completing the remaining steps. We quantified DNA on
149 a Qubit fluorometer and adjusted the concentration to ~13 ng/ μ l; in cases where the
150 concentration was lower than 17 ng/ μ l the concentration was not adjusted. DNA quality was
151 visually assessed on a 2% agarose gel. We submitted genomic DNA for 240 individuals to the
152 Genomics and Bioinformatics Services Texas A&M Agrilife Research centre (College Station, TX)
153 for library preparation using the high-throughput PerkinElmer NEXTFLEX® Rapid XP DNA-Seq Kit

154 and paired-end 150bp sequencing (targeting 10X coverage with ~5.8Gb/sample) on two lanes
155 of a NovaSeq 6000 S4 X.

156

157 ***Alignment and SNP calling***

158 For the whole genome sequences we used bbdduk from the BBTools suite v38.73 for adapter
159 trimming and quality and length filtering (Bushnell, 2021; see code for specific parameters). We
160 aligned whole genome sequences to the *Zostera marina* 3.1 genome (NCBI accession number
161 PRJNA701932; Ma et al., 2021; Olsen et al., 2016) with bwa-mem in bwa v0.7.13 (Li & Durbin,
162 2009) and called SNPs using GATK v. 4.1.0.0 (McKenna et al., 2010). Briefly, we converted sam
163 files to bam format and sorted using samtools v1.9 (Li et al., 2009). Using GATK, we marked
164 duplicates, called haplotypes, combined g.vcf files and then genotyped individuals across
165 batches of 50 (following GATK recommendations for working with large cohort sizes). After
166 retaining only SNPs, we applied additional hard filters for mapping quality, strand bias, variant
167 confidence, and variants with excessive depth following the best practices guidelines in (Van
168 der Auwera et al., 2013; see code for specific parameters). Genotypes for individuals were
169 recoded to missing if they did not have a minimum depth of 10 and a minimum genotype
170 quality score of 30. Although we sampled plants 5-10m apart to limit sampling multiple clonal
171 shoots from the same genet, we also used the SNP data to identify and remove clones, which
172 could confound downstream population genetic analyses. To filter clones from the data set, we
173 used Rclone v1.0.2 (Bailleul, Stoeckel, & Arnaud-Haond, 2016) in R v4.0.3 (R Core Team, 2020)
174 with a reduced set of SNPs without any missing data (as required by the program) for each
175 geographic location separately. After removing clones we used vcftools v0.1.16 (Danecek et al.,

176 2011) to filter the final data set to include only bi-allelic SNPs with a minor allele frequency of at
177 least 0.01 and a genotype call rate of at least 85% of individuals.

178

179 ***Population genetic analyses***

180 For population genetic analysis, we first thinned the SNPs based on linkage disequilibrium (LD)
181 using SNPRelate (Zheng et al., 2012) with an LD threshold of 0.5 based on SNPRelate's
182 "composite" measure of LD. This thinned set was used for clustering analysis, PCA, and F_{ST} . We
183 used SNPRelate to conduct principal components analysis and to calculate pairwise F_{ST} (Weir &
184 Cockerham, 1984) between all pairs of sites. We conducted clustering analysis and estimated
185 ancestry proportions using the R package tess3r (Caye, Deist, Martins, Michel, & François,
186 2016). For each K value (1-6) we ran five replicate runs with the lambda parameter set to 0 to
187 ignore priors based on the spatial distribution of samples.

188

189 ***Sampling water temperature***

190 To record water temperature we deployed HOBO Pendant® MX2201 loggers (fastened to PVC
191 pipe) in the area at each of the sites from which we collected genetic samples. The pipe was
192 driven into the sediment until the logger was approximately <15 cm above the sediment
193 surface, positioned to rarely be emersed except during low spring tides. We recorded water
194 temperature at 15-minute intervals during a two-week period at all sites from August 16th to
195 29th in 2019 and for 14 weeks (Aug 1st – Nov 11th, 2019) for a reduced set of sites that
196 excluded Mason's Marina and one logger at Westside Park in Bodega and Pelican Point and Pita
197 Beach in Tomales Bay. Because our main interest was to determine the relative differences in

198 temperatures between sites, we calculated the mean and first and third quartiles for each
199 location and used Spearman's correlation coefficient to evaluate whether the two-week
200 temperature interval correlated with the longer 14-week interval.

201

202 ***Environmental association analyses***

203 We used two approaches to search for SNPs associated with environmental gradients in
204 Tomales Bay and Bodega Harbor separately: (1) latent factor mixed models (LFMM), correlating
205 individual genotypes at each SNP with mean temperature at the sampling location (Figure 1)
206 using lfmm2 in LEA v4.0.0 (Frichot & François, 2015) and (2) F_{ST} outliers using OutFLANK v0.2
207 (Whitlock & Lotterhos, 2015), grouping warmer vs. cooler sites. For LFMM analysis, genotypes
208 were first imputed in LEA using ancestry coefficients estimated by LEA (K=3). The temperature
209 gradient in Tomales Bay reaches much higher temperatures than that in Bodega Harbor, so to
210 capture a similar range of temperatures for comparisons between bays, we also repeated the
211 analyses with a subset of four sites in Tomales Bay (Lawson's Landing, Pita Beach, Nick's Cove,
212 and Sacramento Landing; Figure 1) that more closely matched the temperature range of
213 Bodega Harbor. We hereafter refer to this reduced Tomales sample as "Tomales (cool)" We also
214 used OutFLANK to identify SNPs associated with higher versus lower intertidal habitat in
215 Bodega. All selection scans were performed after first filtering for SNPs with a minor allele
216 frequency greater than 5% for samples within a given subset of sampling locations. This filter
217 reduces the number of tests performed and discards SNPs unlikely to result in true positives
218 (Caye et al., 2019). Additionally, we assessed outlier SNPs at two different significance cut-offs:
219 $p < 0.001$, a more liberal cutoff without multiple test correction and $q < 0.05$, adjusted for false

220 discovery rate. Because false negatives can be high especially for moderate sample sizes and
221 complex traits, the opportunity to compare across these two significant thresholds provides
222 information about the sensitivity of our conclusions to these decisions.

223 To characterize parallel associations with temperature at the SNP level between the two
224 bays, we directly compared the genomic positions of outlier SNPs from the LFMM and
225 OutFLANK analyses. At the gene level, we used LD-Annot v0.4 with $r^2 = 0.9$ (Prunier et al., 2019)
226 to first identify the genes in linkage disequilibrium with candidate SNPs and then compare lists
227 to detect overlapping genes. Finally, to determine whether there was overlap at the functional
228 level, we tested whether the outlier-associated gene sets were enriched for particular gene
229 ontology (GO) terms using TopGO v2.40.0 (Alexa & Rahnenführer, 2009) in R. We used a
230 possible gene universe of all genes within linkage disequilibrium ($r^2 = 0.9$) of the full set of SNPs,
231 rather than the full set of annotated genes. We used a Fisher's exact test to identify significantly
232 enriched GO terms and required that more than two genes be significant for a particular GO
233 term. We used a significance threshold of $p < 0.05$ and did not adjust for multiple testing, as
234 suggested in (Alexa & Rahnenführer, 2009), as our goal was to summarize the functional
235 categories based on our SNPs rather than to make strong conclusions about any particular GO
236 term.

237 To test predictability of genotype-environment associations within and across bays, we
238 created polygenic scores using the R-package randomForest v4.6-14 (Liaw & Wiener, 2002). We
239 used the mean temperature for each site as the response variable and candidate SNPs derived
240 from LFMM or OutFLANK analyses as predictors. To reduce redundancy and computational
241 time due to extensive linkage across our candidate SNPs, we first thinned the candidate SNP

242 sets based on linkage disequilibrium in SNPRelate (ld.threshold = 0.5). Because randomForest
243 cannot accept missing data, we used genotypes that were imputed with LEA. We ran separate
244 random forest models with the sets of candidate SNPs from LFMM and OutFLANK for each bay.
245 For each SNP set, we conducted runs using either all samples to train the model, or only
246 samples from the bay from which the candidate set was derived (e.g., when candidate SNPs
247 were identified using analysis of Bodega Harbor samples, we trained using either all samples or
248 Bodega Harbor samples only). For validation, we used either all samples, Bodega Harbor only,
249 or Tomales Bay only. To limit bias in the training set, we conducted cross-validation at the level
250 of the sampling site, training the random forest on the dataset with a single sampling site
251 removed, then predicting temperature for that site. For each random forest run, this procedure
252 gave us a random-forest predicted temperature for each individual sample based on candidate
253 SNPs. We then compared predicted and observed temperatures using Spearman's correlation
254 coefficient. For each run, we report the percent variance explained in the training model and
255 the correlation coefficient when comparing observed and predicted temperatures.

256 Because isolation-by-distance is strong in *Z. marina* at this scale in this region (Kamel et
257 al. 2012), we used two approaches to reduce the impacts of IBD driving our predictive power.
258 First, we included in our random forest predictors the sample loadings on the first two PC axes.
259 These first two PC axes represent the major geographical patterns in the system. Second, we
260 ran both training and prediction with 100 random sets of SNPs (in addition to the first two PC
261 axes). We used these randomizations to estimate a 90% confidence interval for a null
262 distribution, showing how well our predictions performed when based on neutral genetic

263 variation alone. When observed variance explained by the random forest model or Spearman's
264 correlation coefficients fell outside this range, we considered them significant.

265

266 **Results**

267

268 ***Genetic variation***

269 After filtering and removing 14 individuals due to low read count, we retained 446,718 SNPs.

270 Where putatively separate samples were identified as clonemates, we retained only one

271 individual from each genet, resulting in 42 additional samples excluded (Table 1, Figure S1). In

272 Tomales Bay, a greater fraction of our samples were identified as clonemates (Figure S1). In the

273 final set of 182 individuals and 446,718 SNPs, 91% of individuals had less than 20% missing

274 data; and all individuals had less than 29% missing genotypes. After thinning for linkage

275 disequilibrium, we were left with 46,166 SNPs for analysis of population structure. Both within

276 and among bays, we found strong isolation by distance (IBD), with pairwise F_{ST} correlated with

277 geographic distance between sites (Figure S3; Spearman's $\rho=0.65$). Differentiation between

278 bays was highest (mean pairwise $F_{ST} = 0.058$, SD = 0.020), and sites within Tomales Bay were

279 more differentiated (mean pairwise $F_{ST} = 0.047$, SD = 0.021) than sites within Bodega Harbor

280 (mean pairwise $F_{ST} = 0.002$, SD = 0.005). Both PCA and clustering analyses supported the IBD

281 pattern (Figure 1), with PC1 and PC2 explaining 4.06% and 1.98%, respectively. Bodega Harbor

282 and Tomales Bay represented distinct clusters on the PCA plot, separated along PC1. PC2

283 mirrored the geography of Tomales Bay, with higher values for sites closer to the mouth of the

284 bay. In the clustering analysis, we observed decreasing cross-validation scores across all values

285 of K, suggesting no clear ‘best’ K value within the range we tested. We present K=3 (Figure 1),
286 as K=4 did not show further geographic differentiation but rather separated five Bodega Harbor
287 individuals. However, at higher K values (K=5,6) additional structure within Tomales Bay
288 became apparent, further highlighting the strong IBD signal (Figure S2).

289

290 ***Environmental association analyses***

291 We documented clear temperature gradients within both Bodega Harbor and Tomales Bay.
292 Summer mean temperatures recorded from 16-29 August in 2019 in Bodega Harbor and
293 Tomales Bay ranged from 16.1–18.5°C and 16.1–22.2°C, respectively, with the mouth of each
294 bay cooler than the back of the bay (Figure 1C; Figure S4). Mean temperatures over this two-
295 week period were highly correlated with an extended period (1 August to 11 November;
296 $\rho=0.95$, $p<2.2e-16$) for which we had logger coverage at all but three sites in Bodega Harbor
297 (two at Mason’s Marina and one at Westside Park) due to logger failure, and all but two sites in
298 Tomales Bay, because the Pelican Point and Pita Beach loggers were not deployed until mid-
299 August (Figure S4). The ordinal ranking of sites by summer temperature reported here is
300 identical to that in other studies of subsets of these sites with longer temperature records (Aoki
301 et al., 2022; DuBois et al., 2022).

302 We identified SNP candidates for selection within each of the two embayments. After
303 filtering for minor allele frequency >5%, 357,010 SNPs remained for environmental association
304 analysis. The vast majority of genetic variation is shared across bays, with only 7,984 SNPs
305 (2.2%) being fixed in one of the bays. Table 2 summarizes the number of SNP outliers at each
306 significance threshold for all analyses. In this discussion and in downstream analyses, unless

307 stated otherwise, we use the false discovery rate-corrected ($q < 0.05$). Bodega Harbor, 8560
308 candidate SNPs were associated with site mean temperature in the LFMM analysis and 314
309 SNPs were significant outliers when comparing the warmest vs. coolest sites in OutFLANK
310 (Figure 2; Table 2). Of the 8472 SNPs identified by LFMM, 8183 (96%) are largely located in a
311 single linked block on Chromosome 1 (Figure 2). Twenty-nine SNPs overlapped between these
312 two analyses. We found 711 genes in linkage disequilibrium with candidate SNPs from the
313 LFMM analysis and 62 from the OutFLANK analysis (see supplementary files), of which 17
314 overlapped between both analyses. Gene enrichment analyses of the candidate genes
315 identified 33 GO terms from LFMM (15 after removing the highly linked region) and 9 from
316 OutFLANK, though none overlapped between the two analyses (Table 2; supplementary files).
317 In the LFMM analysis, significant GO terms included categories broadly involved in cell wall
318 modification, nucleotide metabolism, and enzyme activity while the OutFLANK analysis
319 highlighted categories related to lipid metabolism and heme binding, among others.

320 For Tomales Bay, there were no SNPs significant ($q < 0.05$) when including all Tomales
321 locations. At the unadjusted significance cutoff, 659 candidate SNPs ($p < 0.001$) were associated
322 with mean site temperature across all 10 sampling sites (Table 2; Figure 2). In the LFMM
323 analysis that was restricted to the four coolest sites that most closely matched the temperature
324 gradient of Bodega Harbor, LFMM identified 6710 SNPs ($q < 0.05$) (Figure S5). As with the
325 Bodega Harbor LFMM analysis, the large number of significant SNPs in the reduced Tomales
326 LFMM analysis is largely due to a single highly linked block of SNPs on Chromosome 1; with
327 6256 of 6710 (93%) in that region. The OutFLANK analyses comparing warmer versus cooler
328 sites in Tomales did not yield any candidate SNPs, for either the full 10 sites or the reduced set

329 of four sites. We found 662 genes in linkage disequilibrium with candidate SNPs from the LFMM
330 analysis restricted to only the cooler sites. Twenty GO terms were enriched in the Tomales
331 (cool) LFMM analysis, including nucleic acid and amino acid metabolism functions and enzyme
332 activities. When the linked section of Chromosome 1 was excluded, 21 terms were enriched
333 including functions associated with oxidative stress, carbohydrate metabolism, and organic
334 compound binding.

335

336 **Tidal height associations**

337 The OutFLANK analysis comparing samples from upper and lower tidal heights in Bodega
338 Harbor identified 461 SNPs differentiating the two groups (Table 2, Figure S6, supplementary
339 file). Only one of these SNPs overlapped with other environmental association analysis at the
340 SNP, gene, or functional levels. The unique SNPs differentiating upper and lower intertidal
341 groups were in linkage disequilibrium with 108 genes (Table 2). Gene enrichment analysis found
342 49 enriched GO-terms (Table 2; supplementary files). Most enriched GO terms were generally
343 involved in transcriptional regulation. None of these GO terms overlapped with any of the
344 environment association analyses.

345

346 ***(Non)overlapping associations***

347 There was no overlap in candidate SNPs between Tomales and Bodega Harbor association
348 analyses (Figure 3), with the exception of one highly linked region. Even at a more lenient
349 significance cutoff (unadjusted $p < 0.001$) only 114 candidate SNPs overlapped between
350 embayments, a small fraction (0.8%) of the total 13,360 candidates across all analyses,

351 excluding the highly linked region (Figure S7). There were 5265 significant SNPs that overlapped
352 between the Tomales LFMM analysis restricted to cooler sites and the Bodega LFMM analysis.
353 These SNPs were all located on a single linked region of Chromosome 1 (Figure 2, Figure S5) and
354 so likely represent a single locus. We found 549 genes linked (at LD $r^2 = 0.9$) to candidate SNPs
355 in the Tomales LFMM analysis that was restricted to four cooler sites overlapped with the
356 Bodega OutFlank analysis. After excluding SNPs from the highly linked region, there was still
357 overlap in four genes, despite the absence of overlap at the SNP level. These included a
358 phytochrome interacting factor (PIF1) and endoglucanase, as well as two genes that also were
359 also significant in the more lenient ($p < 0.001$) Tomales LFMM analyses that included all 10
360 locations: UDP-glucuronate:xylan and protein disulfide isomerase.

361 Gene ontology (GO) enrichment analysis for outlier-associated gene sets revealed 14 GO
362 categories that overlapped between the Bodega and Tomales analyses when all SNPs were
363 included. These categories include a range of functions associated with enzyme activity, RNA
364 metabolism, and binding of sugars and phosphates. However, when the large linked region is
365 removed, there are still five functional categories that overlap between Bodega and Tomales
366 (cool) analyses: carbohydrate biosynthetic process, heme binding, UDP-glycosyltransferase
367 activity, transferase activity, and tetrapyrrole binding. Although the large linked block of SNPs
368 represents a prime candidate for follow-up studies, it was not significant in the analysis of all
369 Tomales locations and was only slightly above the significance threshold in the reduced
370 Tomales set. Additionally, both the Bodega and reduced Tomales analyses contain few sites (6
371 in Bodega including high/low intertidal and 4 in Tomales), so further information is needed to
372 test a role for this region in parallel evolution.

373 Polygenic analyses using random forest successfully predicted temperature variation
374 from SNP variation within bays. We used four sets of candidate SNPs that yielded significant
375 candidates for SNPs associated with temperature: Candidates from the three analyses that
376 yielded significant SNPs at $q < 0.05$ (Bodega LFMM, Bodega OutFLANK, and Tomales (cool)
377 LFMM) and an additional set from the full Tomales LFMM at $p < 0.001$, which was included so
378 that we had representation from SNPs that might vary with temperature across the full length
379 of Tomales Bay. We trimmed each SNP set for LD, yielding 175, 61, 121, and 86 SNPs
380 respectively, and used these thinned sets as predictors in the random forest alongside the first
381 two PC axes (to reduce the impact of population structure). Figure 4A-C shows an example run,
382 in which we built the random forest model using SNPs significant in the Bodega LFMM analysis
383 and used all sites in both training and prediction (leaving out one site at a time). In this analysis,
384 the candidate SNPs result in a model with a higher fraction of variance explained ($R^2 = 0.84$) than
385 the same number of random SNPs (90% confidence interval 0.76-0.80). Additionally, the
386 correlation between observed temperature and that predicted by the random forest analysis
387 (Figure 4B) is higher than with a random set of SNPs (Figure 4C; $\rho = 0.80$; 90% CI = 0.62-0.69). In
388 all cases except the Tomales (cool) LFMM, the percent variation explained by the random forest
389 model was significantly higher than with a random set of SNPs. When Tomales Bay sites were
390 used to train the random forest, the null distribution also explained a large percentage of the
391 variance, likely because we included PC axes in the model, which represent the strong isolation
392 by distance in Tomales Bay rather than temperature per se. Still, candidate SNPs rather than
393 random SNPs explained a significantly higher proportion of the variance.

394 Although random forest models performed well when candidate SNP discovery and
395 prediction included only locations within a single embayment, the models did not necessarily
396 perform well when predicting across embayments (Figure 4D). Temperature-associated SNPs
397 discovered in Tomales Bay using LFMM did not predict the temperature at the sites from which
398 Bodega Harbor individuals were collected. Interestingly, random SNPs trained and predicted on
399 Bodega Harbor individuals had a high but negative correlation between observed and predicted
400 temperature (mean LFMM $\rho=-0.72$; OutFLANK $\rho=-0.69$). These negative correlations have been
401 seen in previous studies (Exposito-Alonso et al., 2019), and may reflect an unmeasured
402 environmental variable that is negatively correlated with temperature and with overall
403 population structure. Notably, however, models based on SNPs discovered in Bodega Harbor
404 (both LFMM and OutFLANK) show significantly higher predictive capability than random SNPs,
405 even when predicting the temperature of Tomales Bay sites and regardless of training
406 population.

407 Although the overall success of prediction within embayments and mixed performance
408 across bays is consistent with the lack of parallelism at the SNP level, the significant predictive
409 power of SNPs discovered within the Bodega Harbor candidate SNPs for plants in both
410 embayments suggests that our genome scans may have missed more subtle parallelism. We
411 used the variable importance rankings in the random forest to identify SNPs that contributed
412 most to models trained on Bodega Bay samples, which ultimately resulted in improved
413 predictions of temperature across both bays. Two measures of importance are available within
414 the random forest framework: increase in mean squared error and increase in node purity.
415 Both measures identified three SNPs (one from OutFLANK and two from LFMM) with

416 substantially higher importance than other SNPs or even PC axes (Figure S8), though none
417 overlapped directly with other candidate SNPs from Tomales Bay (Figure 3) or showed linkage
418 with the nearest candidate SNPs (with the range of LD r^2 from 0.001–0.089 at 0.11–6.7 Mb
419 away from the SNPs). Allele frequencies for these SNPs show that they are associated with
420 temperature across both bays and standard linear models indicate a significant correlation with
421 temperature ($p < 0.05$), even when embayment is included as a covariate (Figure S9). Therefore,
422 while the overwhelming conclusion from the genome scans was a lack of parallelism, it appears
423 that the polygenic framework revealed subtle parallel signals.

424

425 Discussion

426 Many factors influence the degree of parallel change in parallel selective environments, such as
427 population size, population history (demographic and genetic), gene flow, environmental
428 heterogeneity, and the fact that there are multiple pathways to the same functional endpoint
429 (Bolnick et al., 2018; Conte et al., 2012; Ralph & Coop, 2015). That all of these vary widely in
430 natural populations at least in part explains the mixed results observed in analyses of
431 parallelism in the wild (Kern & Langerhans, 2018; Oke, Rolshausen, LeBlond, & Hendry, 2017;
432 Stuart et al., 2017). In our study we examine a system in which parallelism would be expected
433 to be likely due to overlapping selective gradients in geographically proximate populations.
434 Counter to this expectation and despite a large degree of shared genetic variation overall, we
435 find that genomic signatures of selection in *Zostera marina* are largely non-overlapping at the
436 SNP level. However, there is detectable overlap in the genes and functional categories
437 associated with temperature variation, and some predictability of temperature across gradients

438 using polygenic scores. Together, these data suggest a complex pattern of subtle parallelism
439 within a mostly non-parallel signal. This supports the emerging view of parallelism as
440 continuous rather than binary (Bolnick et al., 2018).

441 The degree of local adaptation and parallelism can be influenced by the magnitude of
442 gene flow among populations, with migration from nearby populations providing sources of
443 both adaptive and maladaptive genetic variation. We find strong differentiation and isolation by
444 distance among our sample sites, both within and between bays. This is likely due to limited
445 pollen and seed dispersal in *Z. marina* (Ruckelshaus, 1996). Microsatellite studies from Bodega
446 Harbor and Tomales Bay, as well as several other regions, show consistently strong genetic
447 differentiation even at small spatial scales (Campanella et al., 2010; DuBois et al., 2022; Kamel
448 et al., 2012; J. H. Kim et al., 2017; Muñiz-Salazar, Talbot, Sage, Ward, & Cabello-Pasini, 2005;
449 Ort, Cohen, Boyer, & Wyllie-Echeverria, 2012). With limited gene flow to disrupt the effects of
450 selection, local adaptation might occur and be maintained very quickly even at microgeographic
451 scales (Richardson, Urban, Bolnick, & Skelly, 2014).

452 Within each bay, genotype-environment associations were strong, consistent with
453 previous work establishing local adaptation among populations in Tomales Bay. Dubois et al.
454 (DuBois et al., 2022), in a reciprocal transplant that included three of the sites in the present
455 study, documented home-site advantage in survival and growth. Laboratory experiments
456 identified temperature (along with light and grazing pressure) as one of the drivers of local
457 adaptation, with plants from the cool end of the gradient showing decreased performance
458 under elevated temperatures. In Bodega Harbor, temperature-associated SNPs were linked to
459 genes enriched in metabolic processes (e.g., lipid metabolism, oxidation reduction) and cell wall

460 synthesis (e.g., pectinesterase activity, cell wall modification). These perhaps reflect genotype
461 and environment-specific tradeoffs in the use of carbon for growth and metabolism. In Tomales
462 Bay, gene ontology enrichments involved both categories potentially related to growth (e.g.
463 carbohydrate biosynthetic process, cellular carbohydrate metabolic process), but also stress
464 response (e.g. response to oxidative stress, antioxidant activity).

465 Despite evidence for selection across each temperature gradient, there was little
466 overlap in signals of selection at the SNP level. The lack of a pervasive signal of parallelism at
467 the genomic level in the two populations inhabiting Tomales Bay and Bodega Harbor could
468 reflect the impacts of several historical and contemporary evolutionary processes. First, despite
469 their proximity, the two embayments may not be recently derived from the same ancestral
470 population and could instead originate from different sources that had already differentiated to
471 a greater or lesser extent. Second, contemporary gene flow is low between bays (based on our
472 population structure analyses), and even within bays population structure is quite high, likely
473 because of overall limited pollen and seed dispersal (Ruckelshaus, 1996). Beneficial (and
474 deleterious) alleles will thus be slower to spread between bays. Using simulations, Ralph and
475 Coop (2015) demonstrated that in patchy habitats the threshold at which patches are more
476 likely to evolve independent beneficial mutations is a function of dispersal distance and
477 selective advantage of the mutations. In the patchy eelgrass system characteristic of both
478 Tomales Bay and Bodega Harbor, with limited dispersal of pollen and seeds, very strong and
479 persistent selection may be required to enhance the spread of shared adaptive alleles. This is
480 potentially exacerbated by the fact that warmer sites, which exert the strongest selection
481 pressure, are farthest from the mouths of the bays so that when a beneficial allele arises it

482 must pass through less favorable habitat, impeding gene flow to other populations, even those
483 nearby (Ralph & Coop, 2010, 2015).

484 Finally, the range of temperatures within Tomales Bay is much greater than in Bodega
485 Harbor, although we did attempt to reduce the impact of these differences by conducting a
486 reduced analysis based only on overlapping temperature ranges. However, adaptation to other
487 factors besides temperature, whose relative importance may differ between the two
488 embayments, could disrupt parallel signals of selection. For example, seasonal upwelling and
489 phytoplankton and macroalgae blooms are associated with spatially and temporally fluctuating
490 temperature, salinity, chlorophyll, and dissolved oxygen (Hollarsmith et al., 2020; Kimbro,
491 Largier, & Grosholz, 2009). Two of our sites with very similar temperature conditions still
492 exhibited local adaptation to differences in light availability as a result of differences in
493 macroalgal abundance between the sites (DuBois et al., 2021). Although temperature may still
494 impose strong selection, these other sources of selection may constrain the degree of
495 parallelism through, for example through tradeoffs maintained by pleiotropy or epistasis. For
496 example, an analysis of lake-stream pairs of stickleback, although all had adapted across the
497 same primary axis (flow), parallelism was higher when environmental differences were
498 generally more similar (Stuart et al., 2017), highlighting the complexity of multivariate
499 adaptation in wild populations.

500 Even in highly controlled laboratory experiments, parallelism at the genomic level is far
501 from pervasive, suggesting that in natural populations, where ancestry, selective landscapes,
502 and historical and contemporary patterns of gene flow are far more complex, deep parallelism
503 is even less likely (Bailey, Blanquart, Bataillon, & Kassen, 2017; Lenski, 2017). Indeed, a growing

504 number of studies examining adaptation across parallel selection gradients reveal a mix of
505 parallel and non-parallel signals (e.g., Liu et al., 2018; Rivas et al., 2018; Stuart et al., 2017). In
506 our data, despite the overall lack of overlap of signals of selection between the two
507 embayments at the SNP level, there was a small amount of overlap at the gene level and some
508 power for predicting temperature with polygenic scores. Although candidate SNPs from each
509 bay analysed separately had little overlap, the random forest model could still predict Tomales
510 Bay temperatures based on Bodega Harbor candidate SNPs, an unlikely relationship in the
511 absence of any parallel signal.

512 Notably, the most informative SNPs in the random forest model showed correlations
513 between allele frequencies and temperature. These SNPs were perhaps undetected in the
514 genome scan because their effect in Tomales Bay was below the significance threshold; we did
515 not have the power in our study to detect their effects. This is likely a larger issue for detecting
516 parallelism in highly polygenic traits, where we expect small shifts in allele frequencies across
517 many SNPs. Despite the lack of overlap in candidate SNPs, four genes overlapped between
518 Bodega and Tomales analyses, even after we excluded the linked region on Chromosome 1.
519 Since some of the comparisons had no SNP overlap, this may be a case where different
520 mutations in the same gene can lead to comparable phenotypic effects. A similar case was seen
521 in a comparison of small and large morphs of Arctic Charr across multiple lakes in Labrador,
522 where outlier SNPs were largely non-overlapping, but there was overlap at the gene and
523 paralog levels, suggesting multiple mutational pathways to the same functional outcome
524 (Salisbury et al., 2020). In our study, the four genes overlapping between Bodega and Tomales
525 were UDP-glucuronate, protein disulfide isomerase (PDI), an endoglucanase, and PIF1. All of

526 these genes have known functions in plants, many related to growth. Both the endoglucanase
527 and UDP-glucuronate function in cell wall synthesis (Kuang et al., 2016), and PDI and PIF1 are
528 involved in chloroplast regulation and chlorophyll biosynthesis (J. Kim & Mayfield, 1997; Moon,
529 Zhu, Shen, & Huq, 2008). This perhaps points to different genotypes having different light
530 harvesting abilities, which can result in differences in growth and thermal performance. This
531 hypothesis is in line with previous work in *Z. marina* showing genotypic differences in growth
532 under different temperature and seasonal (light) conditions (DuBois et al., 2021). At the
533 functional level, overlapping enriched GO terms between Bodega and Tomales may also be
534 interpreted as associated with growth, including “carbohydrate biosynthesis process” and UDP-
535 glycosyltransferase activity while others, such as “transferase activity” and “tetrapyrrole
536 binding” may be involved in signaling. Additionally, “heme binding” was enriched in both
537 Bodega and Tomales analyses. Hemes play a number of roles in eukaryotic cells, including
538 respiration, transcription, and protein degradation (Severance & Hamza, 2009).

539 The most striking exception to the lack of parallelism was a large region of completely
540 linked SNPs, covering approximately 5Mb on Chromosome 1. These SNPs were significant in
541 both LFMM analyses of Bodega Harbor sites and the four cooler sites in Tomales Bay. We
542 hypothesize that these linked sites represent a chromosomal rearrangement, such as an
543 inversion, that is polymorphic in the sampled populations. Because of the suppressed
544 recombination between alleles, inversions may preserve the integrity of co-adapted gene
545 complexes, which could be especially beneficial when there is gene flow across the selective
546 gradient (Thompson & Jiggins, 2014; Wellenreuther & Bernatchez, 2018). With the increasing
547 accessibility of whole genome sequencing, large inversions appear to be more common than

548 previously thought and may be maintained by selection for a long period (Wellenreuther &
549 Bernatchez, 2018). An interesting case study is that of the seaweed fly *Coelopa frigida*, where
550 inversions are associated with life-history trait variation and show strong and parallel
551 segregation across bioclimatic gradients on two continents (Mérot et al., 2018, 2021). However,
552 links between genotype and environment in our study must be cautiously interpreted because
553 of limited sampling replication across parallel thermal gradients. Further sequencing with long
554 reads will be required to characterize the putative rearrangement. Trait-mapping studies and
555 sampling with broader geographic scope are essential for understanding the fitness
556 consequences of the inversion across different environments.

557 The distribution of climate-associated standing genetic variation in contemporary
558 populations will determine their capacity to adapt to future environmental challenges.
559 However, predictions of future adaptive responses will be aided by an understanding of the
560 genetic architecture of local adaptation (Bay et al., 2017; Capblancq, Fitzpatrick, Bay, Exposito-
561 Alonso, & Keller, 2020). In *Zostera marina* there is mounting evidence that marine heatwaves
562 can reduce growth and reproduction (Ehlers, Worm, & Reusch, 2008; Qin et al., 2020; Saha et
563 al., 2020; Smale et al., 2019), but also that these impacts vary across individuals and
564 populations (Bergmann et al., 2010; DuBois et al., 2019; DuBois, Williams, & Stachowicz, 2020).
565 This study shows strong but largely non-parallel temperature-associated genetic variation
566 across adjacent bays. Whether this is due to a low overall dispersal distance, slowing the spread
567 of adaptive alleles, polygenic adaptation with little overlap in genetic architecture, or
568 populations are adapted to a different suite of complex environmental conditions remains
569 unclear. The distinction is important when considering the loss of genetic variation due to

570 disturbance or when choosing genotypes for restoration: do populations from comparable
571 thermal regimes offer comparably effective sources for restoration of impacted habitats? Our
572 results additionally set expectations for the degree of parallelism we might expect range-wide
573 in *Z. marina*. Our study, which represents conditions likely to generate parallelism (i.e.,
574 geographic proximity, overlapping gradients, contemporary gene flow) shows weakly parallel
575 signals at best, which suggests that parallelism at the genomic level across global *Z. marina*
576 populations is unlikely. Further understanding of the phenotypic effects of candidate SNPs
577 under a range of environmental conditions is essential for understanding how parallel selection
578 shapes the evolutionary trajectories of geographically distinct populations, and for developing a
579 more general framework for predicting individual and population response to warming
580 temperatures.

581

582 **Authors' contributions**

583 L.M.S.: conceptualization, data curation, formal analysis, investigation, methodology, project
584 administration, resources, validation, visualization, writing - original draft, writing - review &
585 editing. R.A.B.: conceptualization, data curation, formal analysis, funding acquisition,
586 investigation, methodology, project administration, resources, supervision, validation,
587 visualization, writing - original draft, writing - review & editing. R.K.G.: conceptualization,
588 funding acquisition, investigation, project administration, resources, supervision, writing -
589 review & editing. J.J.S.: conceptualization, funding acquisition, investigation, methodology,
590 project administration, resources, supervision, writing - review & editing

591

592 Conflict of interest

593 The authors have no conflict of interests.

594

595 Acknowledgements

596 Research was supported by a grant from the U.S. National Science Foundation (OCE-1829976)
597 awarded to R.A.B, R.K.G., and J.J.S. Specimens were collected under scientific collecting permit
598 no. SC-4874 and Specific Use Permit ID: S-211340004-21134-001 from the California
599 Department of Fish & Wildlife and PORE-20I 7-SCI-003 from the National Parks Service. We
600 thank Benjamin Rubinoff for sharing boat time to access Pita Beach and Pelican Point in
601 Tomales Bay. Library prep and sequencing was conducted by Texas A&M AgriLife Research:
602 Genomics and Bioinformatics Service. Sequence processing used the Extreme Science and
603 Engineering Discovery Environment (XSEDE) bridges through allocation and TG-BIO150074 to
604 R.A.B. and TG-OCE200004 to L.M.S., which is supported by National Science Foundation grant
605 number ACI-1548562.

606

607 Data accessibility statement

608 All code, supplementary files, and temperature data are available from the Dryad Digital
609 Repository: <https://doi.org/10.6071/M3DD4F> (Schiebelhut, Grosberg, Stachowicz, & Bay,
610 2022b). Sequence data are available at the NCBI Sequence Read Archive (SRA) under BioProject
611 PRJNA887384 (Schiebelhut, Grosberg, Stachowicz, & Bay, 2022a).

612

613 Benefit-sharing statement

614 Benefits Generated: Benefits from this research accrue from the sharing of our data and results
615 on public databases as described above.

616

617

For Review Only

618 **Tables**

619

620 **Table 1.** List of sample sites, latitude, longitude, sample sizes for genetic analyses, and mean
 621 temperature for *Z. marina* intertidal collections. Sample sizes indicate the final numbers of
 622 individuals included in analyses after filtering out individuals with high missing data and those
 623 that came from the same genet. Parentheses indicate values for lower intertidal samples at
 624 Mason's Marina and Westside Park.
 625

Bay	Site name	Site code	Collection Date	Latitude	Longitude	n	Mean temperature (°C)
Bodega	Mason's Marina	MM	16/Jul/2019; 29/Sep/2019	38.3334	-123.0595	11 (9)	17.4 (17.3)
	Doran Beach	DB	16/Jul/2019; 30/Sep/2019	38.3209	-123.0455	14	18.5
	Westside Park	WP	16/Jul/2019; 29/Sep/2019	38.3195	-123.0538	13 (10)	16.8 (16.4)
	Campbell Cove	CC	16/Jul/2019; 29/Sep/2019	38.3097	-123.0584	12	16.1
Tomales	Lawson's Landing	LL	18/Jul/2019; 27/Sep/2019	38.2303	-122.9588	14	17.3
	Pita Beach	PB	16/Aug/2019	38.2049	-122.9495	7	16.1
	Nick's Cove	NC	01/Aug/2019; 27/Sep/2019	38.2048	-122.9272	14	20.3
	Pelican Point	PP	16/Aug/2019	38.1874	-122.9324	10	16.8
	Blake's Landing	BL	01/Aug/2019; 27/Sep/2019	38.1785	-122.9091	14	20.4
	Sacramento Landing	SL	30/Jul/2019; 26/Sep/2019	38.1496	-122.9056	10	19.8
	Marshall Store	MS	30/Jul/2019; 26/Sep/2019	38.1522	-122.8889	13	20.9
	Heart's Desire	HD	26/Sep/2019; 30/Jul/2019	38.1328	-122.8918	12	20.9
	Teacher's Beach	TB	30/Jul/2019; 26/Sep/2019	38.1141	-122.8694	8	22.0
	Millerton Point	MP	31/Jul/2019; 26/Sep/2019	38.1050	-122.8464	13	22.2

626

627

628

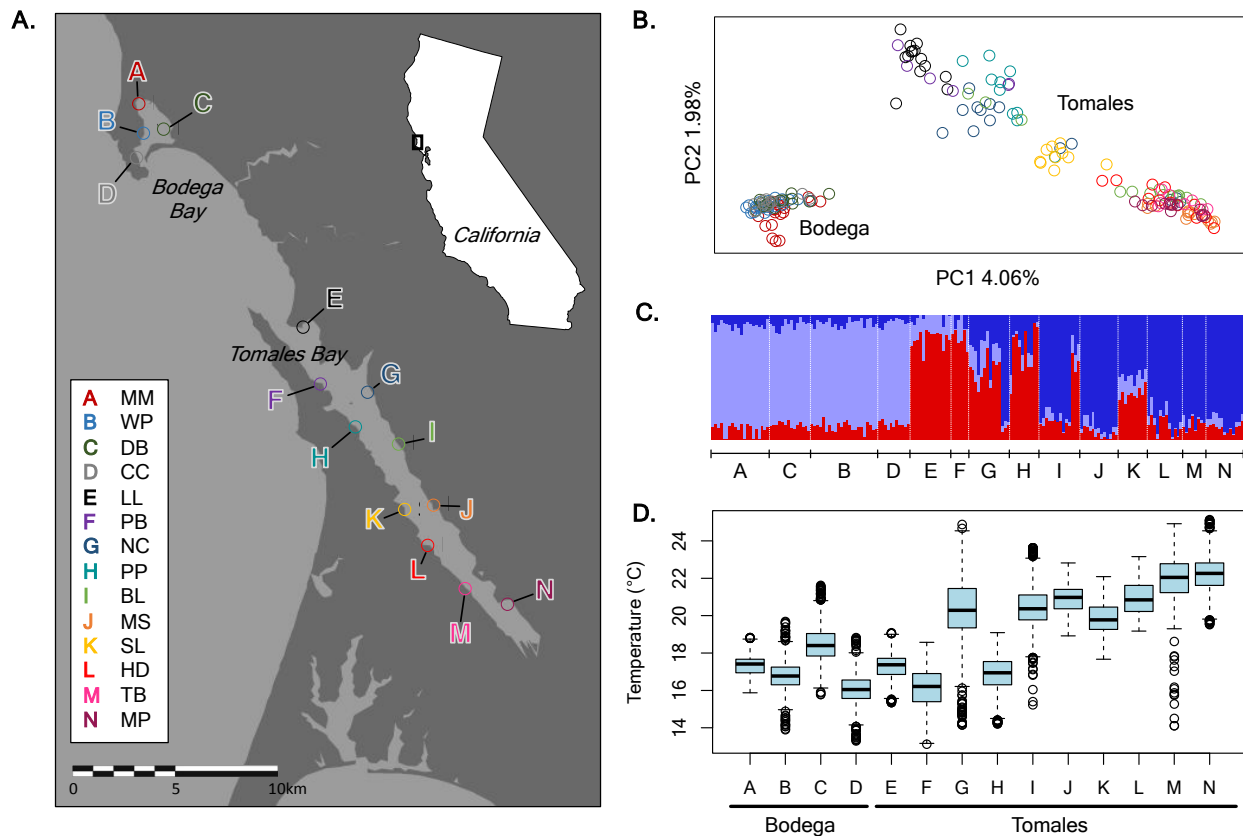
629 **Table 2.** Summary of candidate SNPs from environmental association analyses and linked
 630 genes. Each analysis was conducted for each bay separately. For Tomales Bay, in addition to
 631 using all sites in the LFMM and OutFLANK analyses we also performed the analyses on a
 632 reduced set of four locations that had a temperature profile more closely matching Bodega
 633 Harbor. The number of candidate SNPs are reported for $p < 0.001$ and false discovery rate
 634 adjusted $q < 0.05$. Numbers in parentheses exclude the large linked region on Chromosome 1
 635 (positions 32,368,298–37,501,531). Numbers of candidate genes and functions were evaluated
 636 for SNPs with $q < 0.05$.

637

Bay	Analysis	Candidate SNPs (p -value<0.001)	Candidate SNPs (q value<0.05)	Candidate Genes	Candidate Function
Bodega	LFMM	8472 (289)	8560 (377)	711 (138)	33 (15)
	OutFLANK	4704 (4682)	314	62	9
Tomales	LFMM - all sites	659	0	NA	NA
	OutFLANK - all sites	0	0	NA	NA
	LFMM - cooler sites	6704 (449)	6710 (454)	662 (97)	20 (21)
	OutFLANK - cooler sites	3439 (3411)	0	NA	NA
Bodega	OutFLANK - tidal	4285	461	108	49

638

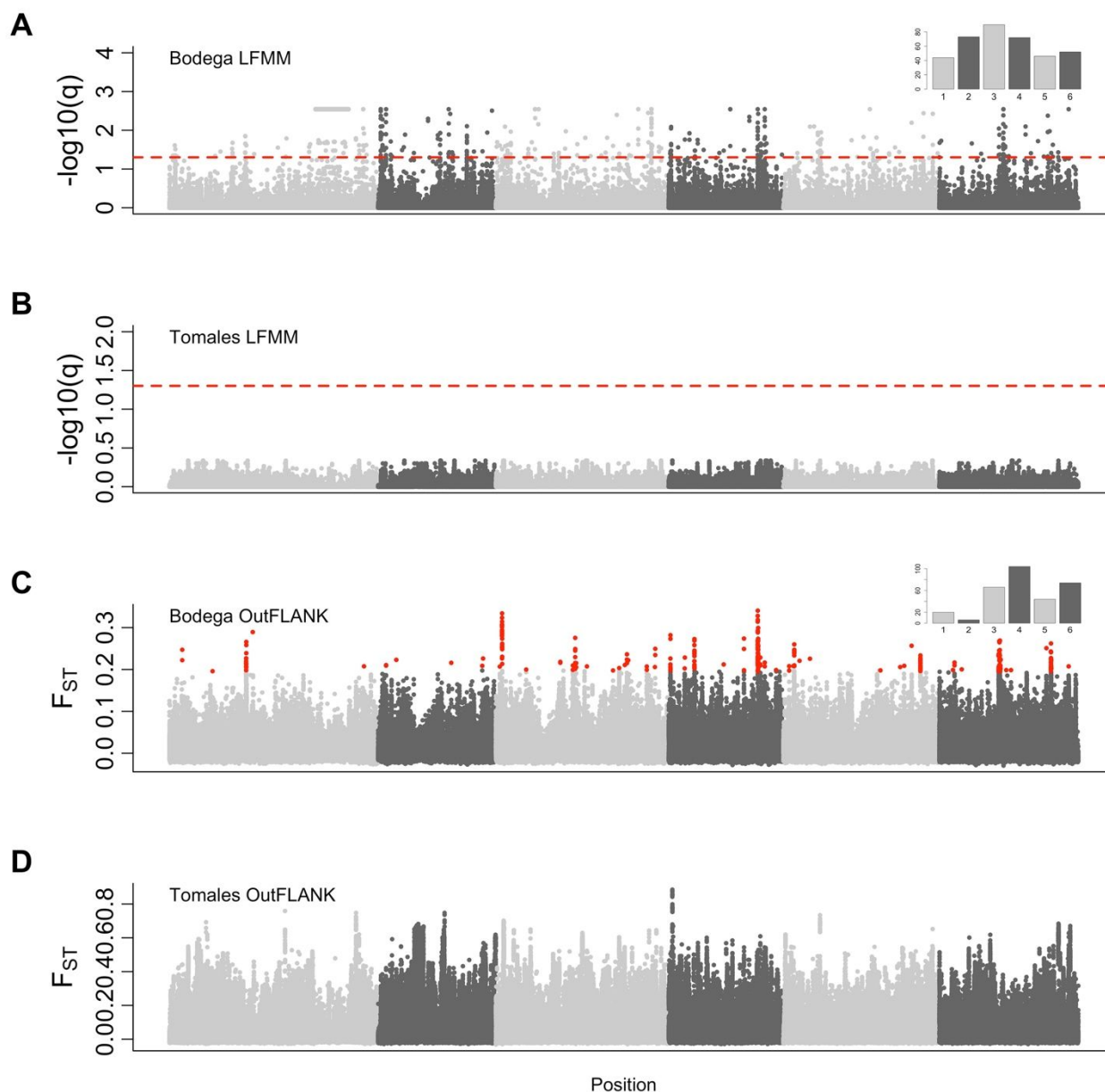
639 **Figures**
 640



641
 642 **Figure 1.** Sampling locations and population genetic structure in *Z. marina*. **(A)** The map
 643 indicates the geographic locations where *Z. marina* were collected and temperature loggers
 644 deployed (see Table 1 for site details and sample sizes). Colored points and letters correspond
 645 to points in the **(B)** PCA. **(C)** Estimated ancestry proportions from clustering analysis ($K=3$) for
 646 each individual, organized by sample site **(D)** Boxplots show the median temperature and first
 647 and third quartiles for each site, as measured over a two-week period in August 2019.

648
 649
 650
 651
 652
 653
 654
 655
 656
 657
 658
 659
 660
 661

662



663
 664 **Figure 2.** Manhattan plots show putative regions of interest from environmental association
 665 analyses using LFMM with average site temperature and OutFLANK comparing warmer versus
 666 cooler sites for Bodega and Tomales separately. For LFMM plots, the red line indicates $p=0.001$
 667 and for the OutFLANK points with $q<0.05$ are highlighted in red. Insets show the number of
 668 outlier SNPs by chromosome, excluding the outliers contained in the large linked region on
 669 Chromosome 1.

670

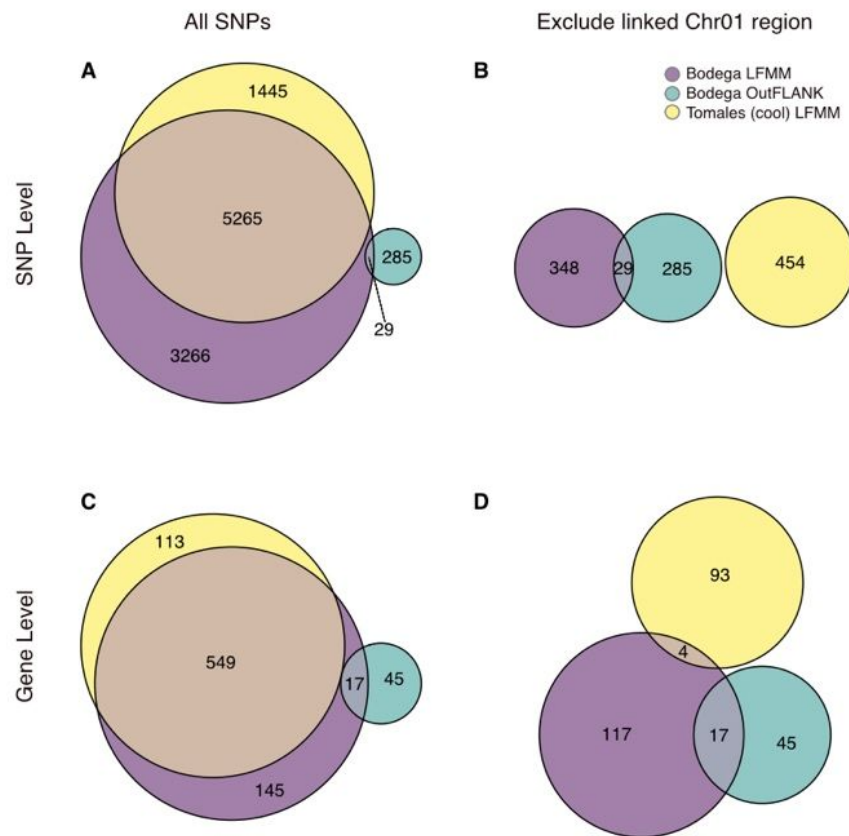
671

672

673

674

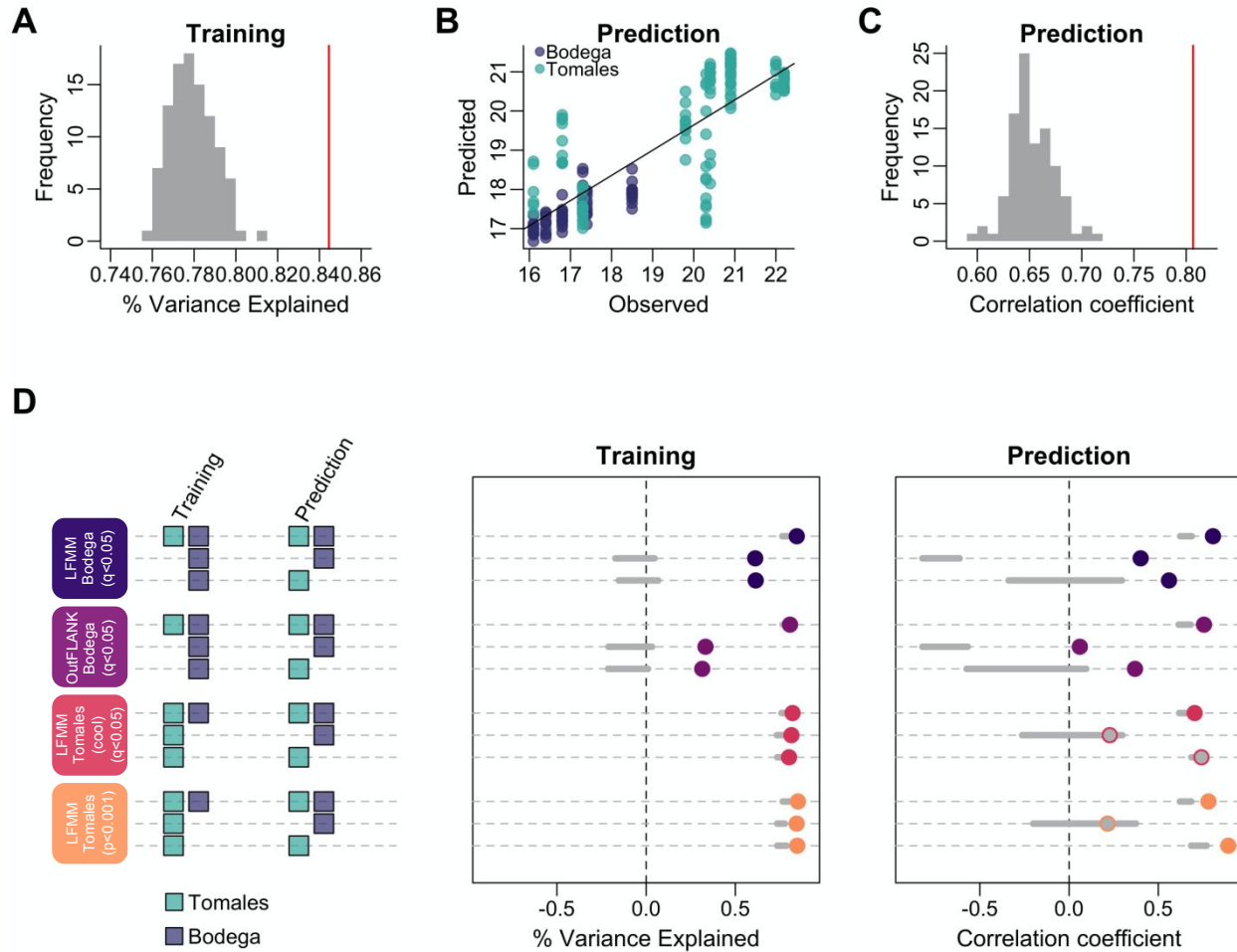
675



676

677

678 **Figure 3.** Overlap among analyses for detecting SNP associations with temperature across two
 679 adjacent embayments. Three sets of candidate SNPs are represented, those detected in Bodega
 680 by LFMM, in Bodega by OutFLANK, and detected in Tomales (cool) by LFMM. Other analyses did
 681 not contain significant SNPs at a threshold of $q < 0.05$. **(A,B)** Overlap at the SNP level for all SNPs
 682 **(A)** and excluding the highly linked region on Chromosome 1 **(B)**. **(C,D)** Overlap in genes linked
 683 to all candidate SNPs **(C)** and excluding the highly linked region on Chromosome 1 **(D)**.



684

685

686 **Figure 4.** Polygenic analysis with random forest suggests limited predictability of thermal687 environment across bays. **(A-C)** An example run showing candidate SNPs from the LFMM688 analysis in Bodega Bay. **(A)** Variance explained by random forest using candidate SNPs as689 predictors (red line) vs. 100 runs with random SNPs (grey histogram). **(B)** Random forest

690 predicted temperatures plotted against observed temperatures for both Bodega and Tomales

691 temperature using candidate SNPs as predictors (red line) vs. 100 runs with random SNPs (grey

692 histogram). **(C)** Correlation coefficients between observed and random forest predicted

693 temperature using candidate SNPs as predictors (red line) vs. 100 runs with random SNPs (grey

694 histogram). **(D)** All combinations of SNP sets and training/prediction populations used in the

695 random forest models. The first panel summarizes which SNP set was used (from top to

696 bottom: LFMM Bodega, OutFLANK Bodega, LFMM Tomales (cool), LFMM Tomales; there is no

697 OutFLANK for Tomales because this analysis did not yield any significant outliers) and which

698 groups were used for training and prediction (i.e., trained using both embayments or only the

699 local embayment to predict Bodega, Tomales, or both). Grey lines are 90% confidence intervals

from the randomizations, filled dots are outside that (i.e., 'significant') and open dots are not

significant.

700 **References**

- 701 Abbott, J. M., DuBois, K., Grosberg, R. K., Williams, S. L., & Stachowicz, J. J. (2018). Genetic
702 distance predicts trait differentiation at the subpopulation but not the individual level in
703 eelgrass, *Zostera marina*. *Ecology and Evolution*, *8*(15), 7476–7489. doi:
704 10.1002/ece3.4260
- 705 Alexa, A., & Rahnenführer, J. (2009). Gene set enrichment analysis with topGO. *Bioconductor*
706 *Improv*, *27*, 1–26.
- 707 Aoki, L. R., Rappazzo, B., Beatty, D. S., Domke, L. K., Eckert, G. L., Eisenlord, M. E., ... Harvell, C.
708 D. (2022). Disease surveillance by artificial intelligence links eelgrass wasting disease to
709 ocean warming across latitudes. *Limnology and Oceanography*, *67*(7), 1577–1589. doi:
710 10.1002/lno.12152
- 711 Arendt, J., & Reznick, D. (2008). Convergence and parallelism reconsidered: what have we
712 learned about the genetics of adaptation? *Trends in Ecology & Evolution*, *23*(1), 26–32. doi:
713 10.1016/j.tree.2007.09.011
- 714 Bailey, S. F., Blanquart, F., Bataillon, T., & Kassen, R. (2017). What drives parallel evolution?:
715 How population size and mutational variation contribute to repeated evolution. *BioEssays:*
716 *News and Reviews in Molecular, Cellular and Developmental Biology*, *39*(1), 1–9. doi:
717 10.1002/bies.201600176
- 718 Bailleul, D., Stoeckel, S., & Arnaud-Haond, S. (2016). RClone: a package to identify MultiLocus
719 Clonal Lineages and handle clonal data sets in r. *Methods in Ecology and Evolution / British*
720 *Ecological Society*, *7*(8), 966–970. doi: 10.1111/2041-210x.12550
- 721 Bay, R. A., Rose, N., Barrett, R., Bernatchez, L., Ghalambor, C. K., Lasky, J. R., ... Ralph, P. (2017).
722 Predicting Responses to Contemporary Environmental Change Using Evolutionary
723 Response Architectures. *The American Naturalist*, *189*(5), 463–473. doi: 10.1086/691233
- 724 Bergmann, N., Winters, G., Rauch, G., Eizaguirre, C., Gu, J., Nelle, P., ... Reusch, T. B. H. (2010).
725 Population-specificity of heat stress gene induction in northern and southern eelgrass
726 *Zostera marina* populations under simulated global warming. *Molecular Ecology*, *19*(14),
727 2870–2883. doi: 10.1111/j.1365-294X.2010.04731.x
- 728 Blount, Z. D., Lenski, R. E., & Losos, J. B. (2018). Contingency and determinism in evolution:
729 Replaying life's tape. *Science*, *362*(6415). doi: 10.1126/science.aam5979
- 730 Bohutínská, M., Vlček, J., Yair, S., Laenen, B., Konečná, V., Fracassetti, M., ... Kolář, F. (2021).
731 Genomic basis of parallel adaptation varies with divergence in *Arabidopsis* and its
732 relatives. *Proceedings of the National Academy of Sciences of the United States of America*,
733 *118*(21). doi: 10.1073/pnas.2022713118
- 734 Bolnick, D. I., Barrett, R. D. H., Oke, K. B., Rennison, D. J., & Stuart, Y. E. (2018). (Non)Parallel
735 Evolution. *Annual Review of Ecology, Evolution, and Systematics*, *49*(1), 303–330. doi:
736 10.1146/annurev-ecolsys-110617-062240
- 737 Bushnell, B. (2021). *BBMap Short Read aligner, and Other Bioinformatic Tools* (Version 38.73).
738 Retrieved from sourceforge.net/projects/bbmap/
- 739 Campanella, J. J., Bologna, P. A. X., Smith, S. M., Rosenzweig, E. B., & Smalley, J. V. (2010).
740 *Zostera marina* population genetics in Barnegat Bay, New Jersey, and implications for grass
741 bed restoration. *Population Ecology*, *52*(1), 181–190. doi: 10.1007/s10144-009-0170-4
- 742 Capblancq, T., Fitzpatrick, M. C., Bay, R. A., Exposito-Alonso, M., & Keller, S. R. (2020). Genomic

- 743 Prediction of (Mal)Adaptation Across Current and Future Climatic Landscapes. *Annual*
744 *Review of Ecology, Evolution, and Systematics*, 51(1), 245–269. doi: 10.1146/annurev-
745 ecolsys-020720-042553
- 746 Cassin-Sackett, L., Callicrate, T. E., & Fleischer, R. C. (2019). Parallel evolution of gene classes,
747 but not genes: Evidence from Hawai’ian honeycreeper populations exposed to avian
748 malaria. *Molecular Ecology*, 28(3), 568–583. doi: 10.1111/mec.14891
- 749 Caye, K., Deist, T. M., Martins, H., Michel, O., & François, O. (2016). TESS3: fast inference of
750 spatial population structure and genome scans for selection. *Molecular Ecology Resources*,
751 16(2), 540–548. doi: 10.1111/1755-0998.12471
- 752 Caye, K., Jumentier, B., Lepeule, J., François, O. (2019) LFMM 2: Fast and Accurate Inference of
753 Gene-Environment Associations in Genome-Wide Studies. *Molecular Biology and*
754 *Evolution*, 36(4), 852–860. <https://doi.org/10.1093/molbev/msz008>
- 755 Conte, G. L., Arnegard, M. E., Peichel, C. L., & Schluter, D. (2012). The probability of genetic
756 parallelism and convergence in natural populations. *Proceedings. Biological Sciences / The*
757 *Royal Society*, 279(1749), 5039–5047. doi: 10.1098/rspb.2012.2146
- 758 Danecek, P., Auton, A., Abecasis, G., Albers, C. A., Banks, E., DePristo, M. A., ... 1000 Genomes
759 Project Analysis Group. (2011). The variant call format and VCFtools. *Bioinformatics* ,
760 27(15), 2156–2158. doi: 10.1093/bioinformatics/btr330
- 761 Doyle, J. J., & Doyle, J. L. (1987). A rapid DNA isolation procedure for small quantities of fresh
762 leaf tissue. *Phytochemical Bulletin*, 19(1), 11–15. Retrieved from
763 <https://worldveg.tind.io/record/33886/>
- 764 DuBois, K., Abbott, J. M., Williams, S. L., & Stachowicz, J. J. (2019). Relative performance of
765 eelgrass genotypes shifts during an extreme warming event: disentangling the roles of
766 multiple traits. *Marine Ecology Progress Series*, 615, 67–77. doi: 10.3354/meps12914
- 767 DuBois, K., Pollard, K. N., Kauffman, B. J., Williams, S. L., & Stachowicz, J. J. (2022). Local
768 adaptation in a marine foundation species: Implications for resilience to future global
769 change. *Global Change Biology*, 28(8), 2596–2610. doi: 10.1111/gcb.16080
- 770 DuBois, K., Williams, S. L., & Stachowicz, J. J. (2020). Previous exposure mediates the response
771 of eelgrass to future warming via clonal transgenerational plasticity. *Ecology*, 101(12),
772 e03169. doi: 10.1002/ecy.3169
- 773 DuBois, K., Williams, S. L., & Stachowicz, J. J. (2021). Experimental Warming Enhances Effects of
774 Eelgrass Genetic Diversity Via Temperature-Induced Niche Differentiation. *Estuaries and*
775 *Coasts*, 44(2), 545–557. doi: 10.1007/s12237-020-00827-9
- 776 Duffy, J. E., Stachowicz, J. J., Reynolds, P. L., Hovel, K. A., Jahnke, M., Sotka, E. E., ... & Olsen, J. L.
777 (2022). A Pleistocene legacy structures variation in modern seagrass
778 ecosystems. *Proceedings of the National Academy of Sciences*, 119(32), e2121425119.
- 779 Ehlers, A., Worm, B., & Reusch, T. B. H. (2008). Importance of genetic diversity in eelgrass
780 *Zostera marina* for its resilience to global warming. *Marine Ecology Progress Series*, 355, 1–
781 7. doi: 10.3354/meps07369
- 782 Exposito-Alonso, M., 500 Genomes Field Experiment Team, Burbano, H. A., Bossdorf, O.,
783 Nielsen, R., & Weigel, D. (2019). Natural selection on the *Arabidopsis thaliana* genome in
784 present and future climates. *Nature*, 573(7772), 126–129. doi: 10.1038/s41586-019-1520-
785 9
- 786 Frichot, E., & François, O. (2015). LEA: An R package for landscape and ecological association

- 787 studies. *Methods in Ecology and Evolution*, 6(8), 925–929. doi: 10.1111/2041-210X.12382
- 788 Hämmerli, A., & Reusch, T. B. H. (2002). Local adaptation and transplant dominance in genets of
789 the marine clonal plant *Zostera marina*. *Marine Ecology Progress Series*, 242, 111–118. doi:
790 10.3354/meps242111
- 791 Härer, A., Bolnick, D. I., & Rennison, D. J. (2021). The genomic signature of ecological divergence
792 along the benthic-limnetic axis in allopatric and sympatric threespine stickleback.
793 *Molecular Ecology*, 30(2), 451–463. doi: 10.1111/mec.15746
- 794 Hollarsmith, J. A., Sadowski, J. S., Picard, M. M. M., Cheng, B., Farlin, J., Russell, A., & Grosholz,
795 E. D. (2020). Effects of seasonal upwelling and runoff on water chemistry and growth and
796 survival of native and commercial oysters. *Limnology and Oceanography*, 65(2), 224–235.
797 doi: 10.1002/lno.11293
- 798 Hughes, A. R., Stachowicz, J. J., & Williams, S. L. (2009). Morphological and physiological
799 variation among seagrass (*Zostera marina*) genotypes. *Oecologia*, 159(4), 725–733. doi:
800 10.1007/s00442-008-1251-3
- 801 Kamel, S. J., Hughes, A. R., Grosberg, R. K., & Stachowicz, J. J. (2012). Fine-scale genetic
802 structure and relatedness in the eelgrass *Zostera marina*. *Marine Ecology Progress Series*,
803 447, 127–137. doi: 10.3354/meps09447
- 804 Kern, E. M. A., & Langerhans, R. B. (2018). Urbanization drives contemporary evolution in
805 stream fish. *Global Change Biology*, 24(8), 3791–3803. doi: 10.1111/gcb.14115
- 806 Kimbro, D. L., Largier, J., & Grosholz, E. D. (2009). Coastal oceanographic processes influence
807 the growth and size of a key estuarine species, the Olympia oyster. *Limnology and*
808 *Oceanography*, 54(5), 1425–1437. doi: 10.4319/lo.2009.54.5.1425
- 809 Kim, J. H., Kang, J. H., Jang, J. E., Choi, S. K., Kim, M. J., Park, S. R., & Lee, H. J. (2017). Population
810 genetic structure of eelgrass (*Zostera marina*) on the Korean coast: Current status and
811 conservation implications for future management. *PloS One*, 12(3), e0174105. doi:
812 10.1371/journal.pone.0174105
- 813 Kim, J., & Mayfield, S. P. (1997). Protein disulfide isomerase as a regulator of chloroplast
814 translational activation. *Science*, 278(5345), 1954–1957. doi:
815 10.1126/science.278.5345.1954
- 816 Kollars, N.M., J.M. Abbott, and J.J. Stachowicz. 2022. Hidden biodiversity: Spatial mosaics of
817 eelgrass genotypic diversity at the centimeter to meadow scale. *Ecology*. doi:
818 10.1002/ecy.3813
- 819 Kuang, B., Zhao, X., Zhou, C., Zeng, W., Ren, J., Ebert, B., ... Wu, A.-M. (2016). Role of UDP-
820 Glucuronic Acid Decarboxylase in Xylan Biosynthesis in *Arabidopsis*. *Molecular Plant*, 9(8),
821 1119–1131. doi: 10.1016/j.molp.2016.04.013
- 822 Lenski, R. E. (2017). Experimental evolution and the dynamics of adaptation and genome
823 evolution in microbial populations. *The ISME Journal*, 11(10), 2181–2194. doi:
824 10.1038/ismej.2017.69
- 825 Liaw, A., & Wiener, M. (2002). Classification and regression by randomForest. *R News*, 2(3), 18–
826 22. Retrieved from
827 [https://www.researchgate.net/file.PostFileLoader.html?id=57d984d196b7e421f8398993&](https://www.researchgate.net/file.PostFileLoader.html?id=57d984d196b7e421f8398993&assetKey=AS%3A406267404275720%401473873105695)
828 [assetKey=AS%3A406267404275720%401473873105695](https://www.researchgate.net/file.PostFileLoader.html?id=57d984d196b7e421f8398993&assetKey=AS%3A406267404275720%401473873105695)
- 829 Li, H., & Durbin, R. (2009). Fast and accurate short read alignment with Burrows-Wheeler
830 transform. *Bioinformatics*, 25(14), 1754–1760. doi: 10.1093/bioinformatics/btp324

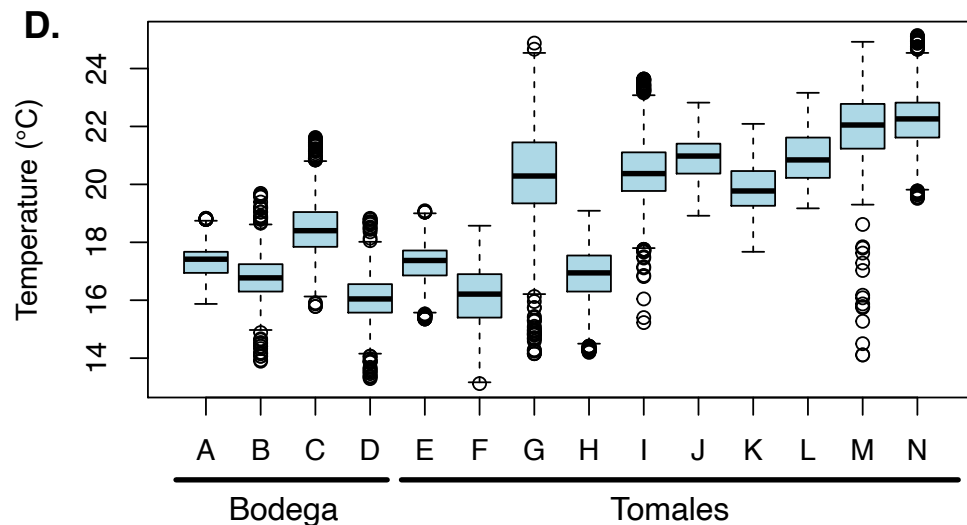
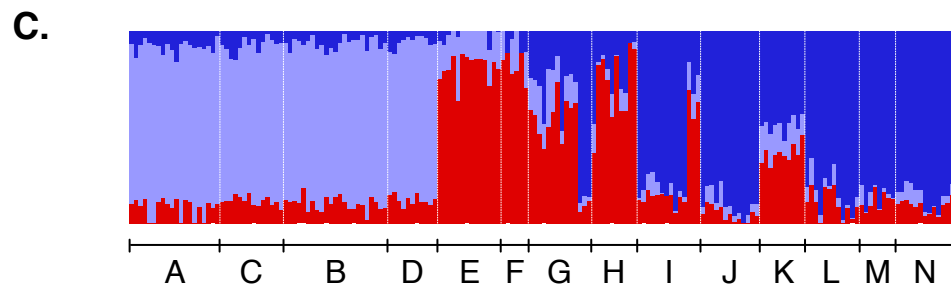
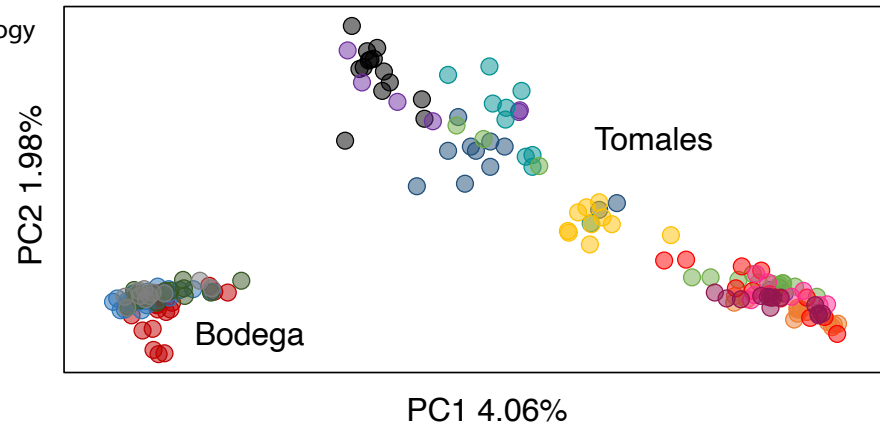
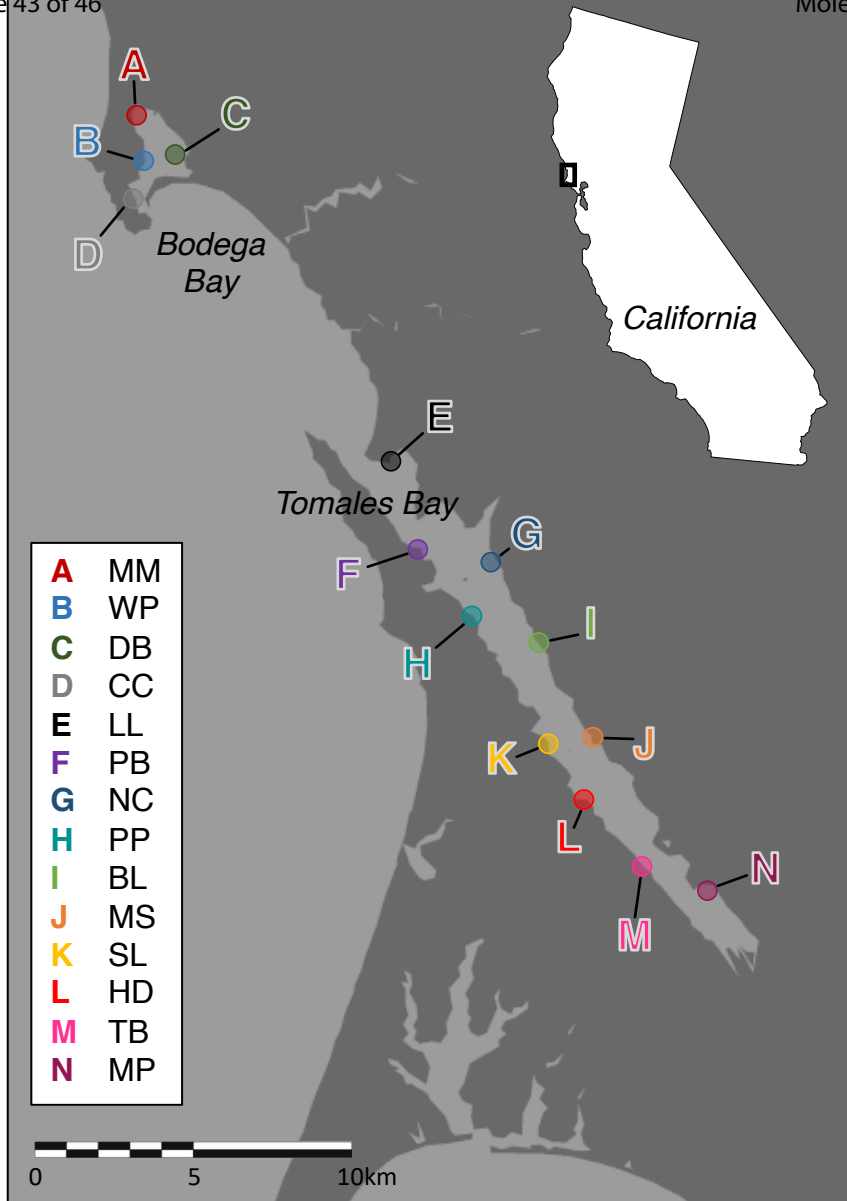
- 831 Li, H., Handsaker, B., Wysoker, A., Fennell, T., Ruan, J., Homer, N., ... 1000 Genome Project Data
832 Processing Subgroup. (2009). The Sequence Alignment/Map format and SAMtools.
833 *Bioinformatics*, 25(16), 2078–2079. doi: 10.1093/bioinformatics/btp352
- 834 Liu, S., Ferchaud, A.-L., Grønkaer, P., Nygaard, R., & Hansen, M. M. (2018). Genomic parallelism
835 and lack thereof in contrasting systems of three-spined sticklebacks. *Molecular Ecology*,
836 27(23), 4725–4743. doi: 10.1111/mec.14782
- 837 Magalhaes, I. S., Whiting, J. R., D'Agostino, D., Hohenlohe, P. A., Mahmud, M., Bell, M. A., ...
838 MacColl, A. D. C. (2021). Intercontinental genomic parallelism in multiple three-spined
839 stickleback adaptive radiations. *Nature Ecology & Evolution*, 5(2), 251–261. doi:
840 10.1038/s41559-020-01341-8
- 841 Ma, X., Olsen, J. L., Reusch, T. B. H., Procaccini, G., Kudrna, D., Williams, M., ... Van de Peer, Y.
842 (2021). Improved chromosome-level genome assembly and annotation of the seagrass,
843 *Zostera marina* (eelgrass) [version 1; peer review: 2 approved]. *F1000Research*, 10, 289.
844 doi: 10.12688/f1000research.38156.1
- 845 McKenna, A., Hanna, M., Banks, E., Sivachenko, A., Cibulskis, K., Kernytsky, A., ... DePristo, M. A.
846 (2010). The Genome Analysis Toolkit: a MapReduce framework for analyzing next-
847 generation DNA sequencing data. *Genome Research*, 20(9), 1297–1303. doi:
848 10.1101/gr.107524.110
- 849 Mérot, C., Berdan, E. L., Babin, C., Normandeau, E., Wellenreuther, M., & Bernatchez, L. (2018).
850 Intercontinental karyotype-environment parallelism supports a role for a chromosomal
851 inversion in local adaptation in a seaweed fly. *Proceedings. Biological Sciences / The Royal*
852 *Society*, 285(1881). doi: 10.1098/rspb.2018.0519
- 853 Mérot, C., Berdan, E. L., Cayuela, H., Djambazian, H., Ferchaud, A.-L., Laporte, M., ... Bernatchez,
854 L. (2021). Locally Adaptive Inversions Modulate Genetic Variation at Different Geographic
855 Scales in a Seaweed Fly. *Molecular Biology and Evolution*, 38(9), 3953–3971. doi:
856 10.1093/molbev/msab143
- 857 Moon, J., Zhu, L., Shen, H., & Huq, E. (2008). PIF1 directly and indirectly regulates chlorophyll
858 biosynthesis to optimize the greening process in *Arabidopsis*. *Proceedings of the National*
859 *Academy of Sciences of the United States of America*, 105(27), 9433–9438. doi:
860 10.1073/pnas.0803611105
- 861 Muñoz-Salazar, R., Talbot, S. L., Sage, G. K., Ward, D. H., & Cabello-Pasini, A. (2005). Population
862 genetic structure of annual and perennial populations of *Zostera marina* L. along the
863 Pacific coast of Baja California and the Gulf of California. *Molecular Ecology*, 14(3), 711–
864 722. doi: 10.1111/j.1365-294X.2005.02454.x
- 865 Oke, K. B., Rolshausen, G., LeBlond, C., & Hendry, A. P. (2017). How Parallel Is Parallel
866 Evolution? A Comparative Analysis in Fishes. *The American Naturalist*, 190(1), 1–16. doi:
867 10.1086/691989
- 868 Olsen, J. L., Rouzé, P., Verhelst, B., Lin, Y.-C., Bayer, T., Collen, J., ... Van de Peer, Y. (2016). The
869 genome of the seagrass *Zostera marina* reveals angiosperm adaptation to the sea. *Nature*,
870 530(7590), 331–335. doi: 10.1038/nature16548
- 871 Olsen, J. L., Stam, W. T., Coyer, J. A., Reusch, T. B., Billingham, M., Boström, C., ... & Wyllie-
872 Echeverria, S. (2004). North Atlantic phylogeography and large-scale population
873 differentiation of the seagrass *Zostera marina* L. *Molecular Ecology*, 13(7), 1923–1941.
- 874 Ort, B. S., Cohen, C. S., Boyer, K. E., & Wyllie-Echeverria, S. (2012). Population structure and

- 875 genetic diversity among eelgrass (*Zostera marina*) beds and depths in San Francisco Bay.
876 *The Journal of Heredity*, 103(4), 533–546. doi: 10.1093/jhered/ess022
- 877 Pickersgill, B. (2018). Parallel vs. Convergent Evolution in Domestication and Diversification of
878 Crops in the Americas. *Frontiers in Ecology and Evolution*, 6. doi: 10.3389/fevo.2018.00056
- 879 Prunier, J., Lemaçon, A., Bastien, A., Jafarikia, M., Porth, I., Robert, C., & Droit, A. (2019). LD-
880 annot: A Bioinformatics Tool to Automatically Provide Candidate SNPs With Annotations
881 for Genetically Linked Genes. *Frontiers in Genetics*, 10, 1192. doi:
882 10.3389/fgene.2019.01192
- 883 Qin, L.-Z., Kim, S. H., Song, H.-J., Kim, H. G., Suonan, Z., Kwon, O., ... Lee, K.-S. (2020). Long-term
884 variability in the flowering phenology and intensity of the temperate seagrass *Zostera*
885 *marina* in response to regional sea warming. *Ecological Indicators*, 119, 106821. doi:
886 10.1016/j.ecolind.2020.106821
- 887 Ralph, P., & Coop, G. (2010). Parallel adaptation: one or many waves of advance of an
888 advantageous allele? *Genetics*, 186(2), 647–668. doi: 10.1534/genetics.110.119594
- 889 Ralph, P., & Coop, G. (2015). Convergent Evolution During Local Adaptation to Patchy
890 Landscapes. *PLoS Genetics*, 11(11), e1005630. doi: 10.1371/journal.pgen.1005630
- 891 R Core Team. (2020). *R: A language and environment for statistical computing*. Vienna, Austria.
- 892 Rennison, D. J., Delmore, K. E., Samuk, K., Owens, G. L., & Miller, S. E. (2020). Shared Patterns of
893 Genome-Wide Differentiation Are More Strongly Predicted by Geography Than by Ecology.
894 *The American Naturalist*, 195(2), 192–200. doi: 10.1086/706476
- 895 Reusch, T. B. H., Stam, W. T. & Olsen, J. L. (1999) Microsatellite loci in eelgrass *Zostera marina*
896 reveal marked polymorphism within and among populations. *Molecular Ecology*, 8, 317–
897 322.
- 898 Reynolds, L. K., DuBois, K., Abbott, J. M., Williams, S. L., & Stachowicz, J. J. (2016). Response of a
899 Habitat-Forming Marine Plant to a Simulated Warming Event Is Delayed, Genotype
900 Specific, and Varies with Phenology. *PloS One*, 11(6), e0154532. doi:
901 10.1371/journal.pone.0154532
- 902 Reynolds, L.K., Stachowicz, J.J., Hughes, A.R., Kamel, S.J., Ort, B. and R.H. Grosberg. (2017).
903 Temporal stability in patterns of genetic diversity and structure of a marine foundation
904 species (*Zostera marina*). *Heredity*, 118:404–412.
- 905 Richardson, J. L., Urban, M. C., Bolnick, D. I., & Skelly, D. K. (2014). Microgeographic adaptation
906 and the spatial scale of evolution. *Trends in Ecology & Evolution*, 29(3), 165–176. doi:
907 10.1016/j.tree.2014.01.002
- 908 Rivas, M. J., Saura, M., Pérez-Figueroa, A., Panova, M., Johansson, T., André, C., ... Quesada, H.
909 (2018). Population genomics of parallel evolution in gene expression and gene sequence
910 during ecological adaptation. *Scientific Reports*, 8(1), 16147. doi: 10.1038/s41598-018-
911 33897-8
- 912 Roda, F., Ambrose, L., Walter, G. M., Liu, H. L., Schaul, A., Lowe, A., ... Ortiz-Barrientos, D.
913 (2013). Genomic evidence for the parallel evolution of coastal forms in the *Senecio lautus*
914 complex. *Molecular Ecology*, 22(11), 2941–2952. doi: 10.1111/mec.12311
- 915 Rosenblum, E. B., Römler, H., Schöneberg, T., & Hoekstra, H. E. (2010). Molecular and
916 functional basis of phenotypic convergence in white lizards at White Sands. *Proceedings of*
917 *the National Academy of Sciences of the United States of America*, 107(5), 2113–2117. doi:
918 10.1073/pnas.0911042107

- 919 Ruckelshaus, M. H. (1996). Estimation of genetic neighborhood parameters from pollen and
920 seed dispersal in the marine angiosperm *Zostera marina* L. *Evolution; International Journal*
921 *of Organic Evolution*, 50(2), 856–864. doi: 10.1111/j.1558-5646.1996.tb03894.x
- 922 Saha, M., Barboza, F. R., Somerfield, P. J., Al-Janabi, B., Beck, M., Brakel, J., ... Sawall, Y. (2020).
923 Response of foundation macrophytes to near-natural simulated marine heatwaves. *Global*
924 *Change Biology*, 26(2), 417–430. doi: 10.1111/gcb.14801
- 925 Salisbury, S. J., McCracken, G. R., Perry, R., Keefe, D., Layton, K. K. S., Kess, T., ... Ruzzante, D. E.
926 (2020). Limited genetic parallelism underlies recent, repeated incipient speciation in
927 geographically proximate populations of an Arctic fish (*Salvelinus alpinus*). *Molecular*
928 *Ecology*, 29(22), 4280–4294. doi: 10.1111/mec.15634
- 929 Salo, T., Reusch, T. B. H., & Boström, C. (2015). Genotype-specific responses to light stress in
930 eelgrass *Zostera marina*, a marine foundation plant. *Marine Ecology Progress Series*, 519,
931 129–140. doi: 10.3354/meps11083
- 932 Schiebelhut, L. M., Grosberg, R. K., Stachowicz, J. J., & Bay, R. A. (2022a). *BioProject*
933 *PRJNA887384*. National Center for Biotechnology Information Sequence Read Archive [Data
934 set]. Retrieved from <http://www.ncbi.nlm.nih.gov/bioproject/887384>
- 935 Schiebelhut, L. M., Grosberg, R. K., Stachowicz, J. J., & Bay, R. A. (2022b). *Data and code*
936 *associated with “Genomic responses to parallel selection in the eelgrass *Zostera marina* in*
937 *adjacent bays”*. *Dryad Digital Repository* [Data set]. [Dryad Digital Repository](https://doi.org/10.6071/M3DD4F).
938 <https://doi.org/10.6071/M3DD4F>
- 939 Severance, S., & Hamza, I. (2009). Trafficking of heme and porphyrins in metazoa. *Chemical*
940 *Reviews*, 109(10), 4596–4616. doi: 10.1021/cr9001116
- 941 Smale, D. A., Wernberg, T., Oliver, E. C. J., Thomsen, M., Harvey, B. P., Straub, S. C., ... Moore, P.
942 J. (2019). Marine heatwaves threaten global biodiversity and the provision of ecosystem
943 services. *Nature Climate Change*, 9(4), 306–312. doi: 10.1038/s41558-019-0412-1
- 944 Stuart, Y. E. (2019). Divergent Uses of “Parallel Evolution” during the History of The American
945 Naturalist. *The American Naturalist*, 193(1), 11–19. doi: 10.1086/700718
- 946 Stuart, Y. E., Veen, T., Weber, J. N., Hanson, D., Ravinet, M., Lohman, B. K., ... Bolnick, D. I.
947 (2017). Contrasting effects of environment and genetics generate a continuum of parallel
948 evolution. *Nature Ecology & Evolution*, 1(6), 158. doi: 10.1038/s41559-017-0158
- 949 Szendro, I. G., Franke, J., de Visser, J. A. G. M., & Krug, J. (2013). Predictability of evolution
950 depends nonmonotonically on population size. *Proceedings of the National Academy of*
951 *Sciences of the United States of America*, 110(2), 571–576. doi: 10.1073/pnas.1213613110
- 952 Tenaillon, O., Rodríguez-Verdugo, A., Gaut, R. L., McDonald, P., Bennett, A. F., Long, A. D., &
953 Gaut, B. S. (2012). The molecular diversity of adaptive convergence. *Science*, 335(6067),
954 457–461. doi: 10.1126/science.1212986
- 955 Thompson, M. J., & Jiggins, C. D. (2014). Supergenes and their role in evolution. *Heredity*,
956 113(1), 1–8. doi: 10.1038/hdy.2014.20
- 957 Van der Auwera, G. A., Carneiro, M. O., Hartl, C., Poplin, R., Del Angel, G., Levy-Moonshine, A.,
958 ... DePristo, M. A. (2013). From FastQ data to high confidence variant calls: the Genome
959 Analysis Toolkit best practices pipeline. *Current Protocols in Bioinformatics / Editorial*
960 *Board, Andreas D. Baxevanis ... [et Al.]*, 43, 11.10.1–11.10.33. doi:
961 10.1002/0471250953.bi1110s43
- 962 Weir, B. S., & Cockerham, C. C. (1984). Estimating F-Statistics for the Analysis of Population

- 963 Structure. *Evolution; International Journal of Organic Evolution*, 38(6), 1358–1370. doi:
964 10.2307/2408641
- 965 Wellenreuther, M., & Bernatchez, L. (2018). Eco-Evolutionary Genomics of Chromosomal
966 Inversions. *Trends in Ecology & Evolution*, 33(6), 427–440. doi: 10.1016/j.tree.2018.04.002
- 967 Whitlock, M. C., & Lotterhos, K. E. (2015). Reliable Detection of Loci Responsible for Local
968 Adaptation: Inference of a Null Model through Trimming the Distribution of F_{ST} . *The*
969 *American Naturalist*, 186 Suppl 1, S24–S36. doi: 10.1086/682949
- 970 Yu, L., Stachowicz, J.J., Dubous, K. and Reusch, T.B.H. (2022). Detecting clonemate pairs in
971 multicellular diploid clonal species based on a shared heterozygosity index. *Molecular*
972 *Ecology Resources*, doi: 10.1111/1755-0998.13736
- 973 Zheng, X., Levine, D., Shen, J., Gogarten, S. M., Laurie, C., & Weir, B. S. (2012). A high-
974 performance computing toolset for relatedness and principal component analysis of SNP
975 data. *Bioinformatics*, 28(24), 3326–3328. doi: 10.1093/bioinformatics/bts606

For Review Only



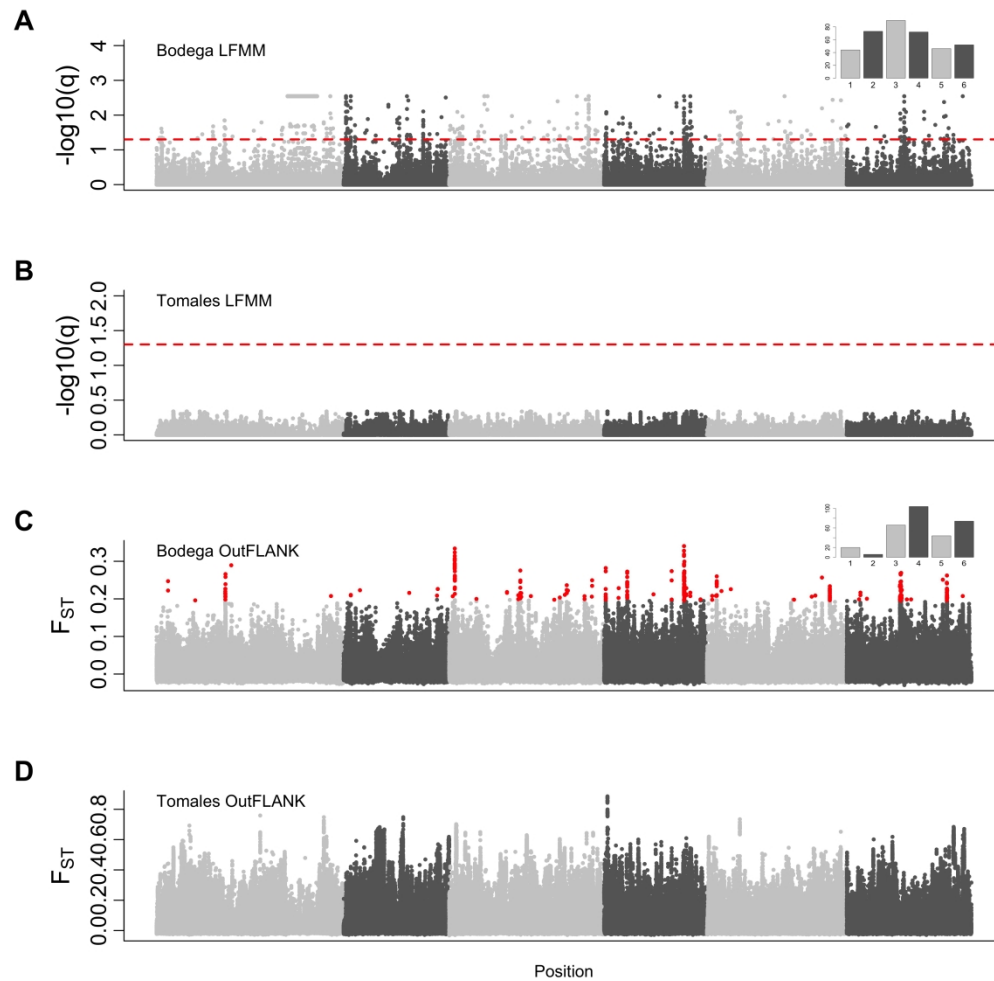


Figure 2. Manhattan plots show putative regions of interest from environmental association analyses using LFMM with average site temperature and OutFLANK comparing warmer versus cooler sites for Bodega and Tomales separately. For LFMM plots, the red line indicates $p=0.001$ and for the OutFLANK points with $q < 0.05$ are highlighted in red. Insets show the number of outlier SNPs by chromosome, excluding the outliers contained in the large linked region on Chromosome 1.

1763x1763mm (72 x 72 DPI)

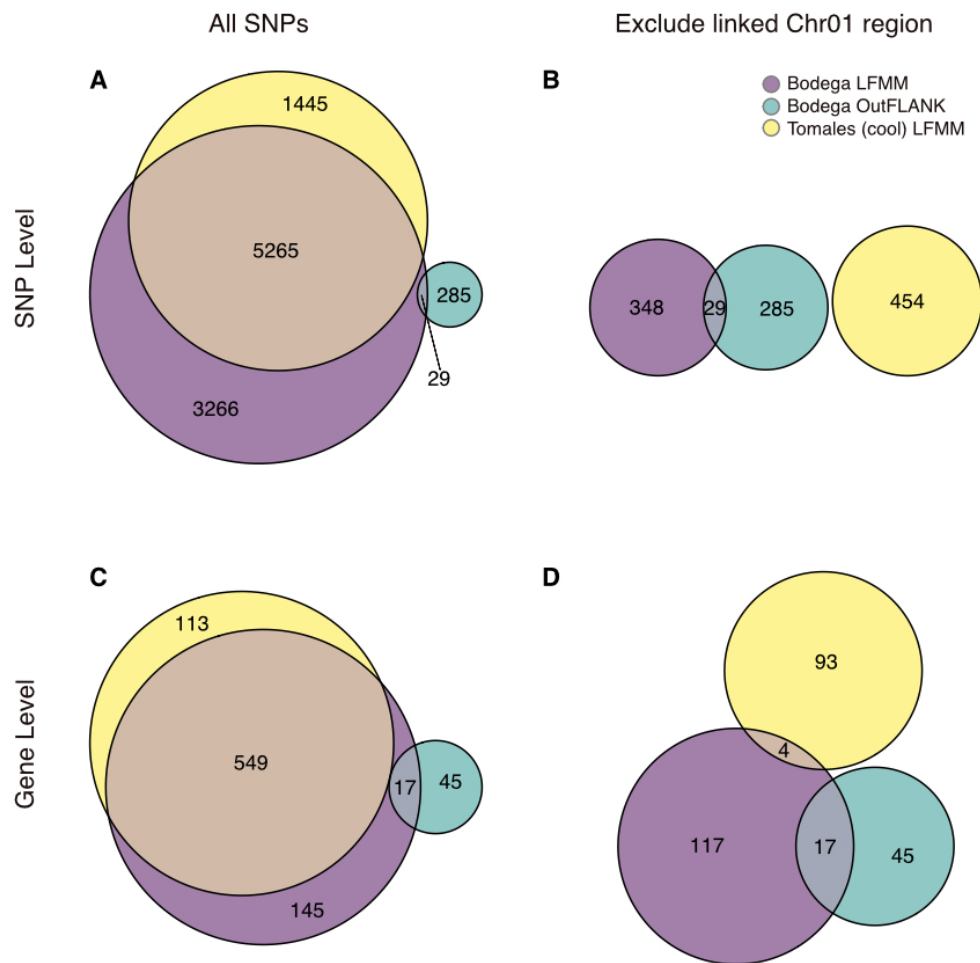


Figure 3. Overlap among analyses for detecting SNP associations with temperature across two adjacent embayments. Three sets of candidate SNPs are represented, those detected in Bodega by LFMM, in Bodega by OutFLANK, and detected in Tomales (cool) by LFMM. Other analyses did not contain significant SNPs at a threshold of $q < 0.05$. (A,B) Overlap at the SNP level for all SNPs (A) and excluding the highly linked region on Chromosome 1 (B). (C,D) Overlap in genes linked to all candidate SNPs (C) and excluding the highly linked region on Chromosome 1 (D).

304x304mm (72 x 72 DPI)

